Heavy-mineral provenance signatures during the infill and uplift of a foreland basin: an example from the Jaca basin (Southern Pyrenees, Spain)

XAVIER COLL[1], DAVID GÓMEZ-GRAS[1], MARTA ROIGÉ[1], ANTONIO TEIXELL[1], SALVA BOYA[1], AND NARCÍS MESTRES[2]

[1]Departament de Geologia, Universitat Autònoma de Barcelona, 08193 Bellaterra, Spain

[2]Institut de Ciència de Materials de Barcelona, ICMAB, Consejo Superior de Investigaciones Científicas, CSIC, Campus de la UAB 08193 Bellaterra, Barcelona, Spain

e-mail: Xavier.Coll@uab.cat

ABSTRACT

In the Jaca foreland basin (Southern Pyrenees), two main sediment routing systems merge from the late Eocene to the early Miocene, providing an excellent example of interaction of different source areas with distinct petrographic signatures. An axially drained fluvial system, with its source area located in the eastern Central Pyrenees, is progressively replaced by a transverse-drained system that leads to the recycling of the older turbiditic foredeep. Aiming to provide new insights into the source-area evolution of the Jaca foreland basin, we provide new data on heavy-mineral suites, from the turbiditic underfilled stage to the youngest alluvial-fan systems of the Jaca basin, and integrate the heavy-mineral signatures with available sandstone petrography. Our results show a dominance of the ultrastable Ap-Zrn-Tur-Rt assemblage through the entire basin evolution. However, a late alluvial sedimentation stage brings an increase in other more unstable heavy minerals, pointing to specific source areas belonging to the Axial and the North Pyrenean Zone and providing new insights into the response of the heavy-mineral suites to sediment recycling. Furthermore, we assess the degree of diagenetic overprint vs. provenance signals and infer that the loss of unstable heavy minerals due intrastratal dissolution is negligible at least in the Peña Oroel and San Juan de la Peña sections. Finally, we provide new evidence to the idea that during the late Eocene the water divide of the transverse drainage system was located in the North Pyrenean Zone, and areas constituted by the Paleozoic basement were exposed in the west-Central Pyrenees at that time. Our findings provide new insights into the heavy-mineral response in recycled foreland basins adjacent to fold-and-thrust belts.

INTRODUCTION

The sedimentary infill of a foreland basin may record the interaction of distinct source areas, thus offering a good chance to study the interplay between them and to infer the evolution of the uplift and exhumation of mountain belts (e.g., Dickinson and Suczek 1979; Steidtmann and Schmitt 1988). Sediment provenance studies are important to understand the processes occurring in the hinterland of a sedimentary basin, helping to constrain the timing of geodynamic events, to unravel sediment pathways, and to correlate stratigraphic sequences (Graham et al. 1986; Haughton et al. 1991; Mange-Rajetzky 1995; Von Eynatten and Dunkl 2012; Garzanti et al. 2013a, 2013b; Kilhams et al. 2014; Caracciolo et al. 2016). In complex geodynamic settings, the integration of as many provenance tools as possible is essential to resolve ambiguous provenance signals when facing sediment routing in related basins (Dickinson 1988; Nie et al. 2012; Garzanti et al. 2013a; Garzanti 2016; Caracciolo et al. 2019; McKellar et al. 2020).

The use of heavy minerals to assess sediment provenance in source-to-sink studies has been proven as a powerful tool in many basins and different settings (Morton et al. 1994, 2004; von Eynatten 1999; Mange et al. 2003; Garzanti and Andò 2007b; Garzanti et al. 2007, 2013a, 2014; Fossum et al. 2019). Different sources can be revealed in sediments with similar petrographic compositions through the study of the heavy-mineral suites (Mange-Rajetzky 1995). However, since ancient sandstones are usually affected by intrastratal dissolution (Morton and Hallsworth 1999, 2007; Andò et al. 2012), most studies tend to focus on modern sediments (Garzanti et al. 2003, 2013a, 2013b, 2014, 2018; Garzanti and Andò 2007a, 2007b). In addition, interpreting heavy-mineral suites without contrasting to petrographic data may lead to misleading conclusions, especially when the degree of diagenetic overprint is enough to substantially modify the original detrital suite.

The Eocene-Miocene Jaca foreland basin of the Southern Pyrenees (Fig. 1) has been thoroughly studied regarding sedimentology, tectonics, and petrography (Mutti 1985; Mutti et al. 1985; Remacha and Fernández 2003; Remacha et al. 2005; Caja et al. 2010; Fontana et al. 1989; Gupta and Pickering 2008; Labaume et al. 1985, 2016a; Labaume and Teixell 2018; Roigé et al., 2016, 2017; Boya 2018, Garcés et al. 2020) as it is an outstanding example of a basin infill evolving in an active convergent tectonic setting. Different sediment routing systems merge in this basin, providing an example of interaction of different source areas with distinct petrographic signatures, recording several stages of exhumation of the Pyrenean belt (Puigdefàbregas 1975; Roigé et al. 2016, 2017). The well-constrained geological setting of the Jaca basin offers an excellent opportunity to test how heavy-mineral suites respond to changes in the sediment routing system, the sedimentary environment (from deep-marine to terrestrial), and the potential diagenetic overprint.

Despite the wide use of heavy minerals as provenance indicators in other orogens such as the Alps or the Himalayas (Cerveny et al. 1989; Lihou and Mange-Rajetzky 1996; von Eynatten and Gaupp 1999; Garzanti et al. 2004, 2006, 2012, 2013a; Uddin et al. 2007; Andò et al. 2014, 2019), in the Pyrenees few or mainly old studies have used this approach to unravel sediment provenance in the South-Pyrenean and the Ebro basin (Ullastre and Masriera 1982; Hirst and Nichols 1986; Rubio et al. 1996; Yuste et al. 2006; Barsó 2007; Michael 2013; Gómez-Gras et al. 2017). In the Ainsa-Jaca basin, only Valloni et al. (1984) and Coll et al. (2017) addressed the study of heavy minerals in the intensely studied Eocene turbidites of the Hecho Group (Mutti 1985), leading to strongly different results.

We provide new characterization of the heavy-mineral suites of the clastic systems of the northern Jaca basin, from the deep-marine sedimentation stage to the latest stage of its continentalization (Late Lutetian-Miocene), in order to unravel provenance signatures and to gain understanding of the degree of diagenetic overprint throughout the study area. In addition, we aim to provide new insights into the sediment-routing responses to the creation of new drainage patterns during the uplift and topographic growth of the Pyrenees, through the integration of heavy-mineral analysis with available sandstone petrography data (Roigé et al. 2016, 2017).

GEOLOGICAL SETTING

Structural and Stratigraphic Framework

From the late Cretaceous until the early Miocene, the collision between the Eurasian and Iberian plates originated the Pyrenean fold-and-thrust belt (Roure et al. 1989; Muñoz 1992; Teixell 1998; Vergés et al. 2002; Mouthereau et al. 2014). As the lower crust of the Iberian plate was subducted under the European plate, a doubly vergent orogenic prism developed diachronously from east to west in the upper crust, leading to the inversion of the former Mesozoic basin and the stacking of the basement. Inverted hyper-extensional Mesozoic basins constitute the North Pyrenean Zone (Lagabrielle et al 2010), bordered to the north by the Aquitanian basin (Fig.1). Conversely, the Southern Pyrenees consists of a thrust fan that is constituted by four main thrust sheets in the west-central Pyrenees (Teixell 1996; Labaume et al. 2016a). These are the Lakora-Eaux-Chaudes, Gavarnie, Broto, and Guarga thrust sheets, which involve the Paleozoic basement, a preorogenic Mesozoic succession, and the Cretaceous to early Miocene foreland basin. The late Santonian to early Miocene synorogenic sequence constitutes the detached South Pyrenean foreland basin (including the Jaca basin), separated by the autochtonous Ebro basin to the south by the thrust front of the External Sierras.

During the Eocene, the Ager and Tremp-Graus basins of the east-central Pyrenees concentrated the fluvio-deltaic environments, funnelling sediments to the west, to the slope and deep-marine Ainsa and Jaca basins, where a thick turbidite succession known as the Hecho Group was deposited in the Jaca basin (Nijman and Nio 1975; Mutti 1985; Puigdefàbregas et al. 1992; Caja et al. 2010; Garcés et al. 2020). The lower to middle Eocene deep-marine turbiditic sedimentation stage was axially fed from the east, with its source area located in the uplifting central Pyrenees and the Ebro Massif to the south (Caja et al. 2010; Roigé et al. 2016; Gómez-Gras et al. 2016). Nevertheless, a provenance shift occurred during the last turbidite-sedimentation stage (the Rapitán channel, Remacha et al. 1995), evidenced by a change in paleocurrents, facies, and sediment composition, that recorded the first north derived sediments from new emerged source areas (Roigé et al. 2016). In the Bartonian, the shallow marine and transitional environments replaced the deep-marine sedimentation, and the basin depocenter migrated to the south (Oms et al. 2003; Teixell 1996). The Larrés Marls and the Sabiñanigo sandstone Formation are the first delta-slope and delta-front sediments recorded in the basin (Puigdefàbregas 1975; Boya 2018), followed by the Pamplona Marls (Mangin 1960) and the delta front of the Priabonian Belsué-Atarés sandstone Formation.

The growth of fold structures in the Jaca basin (Puigdefàbregas 1975; Hogan 1993; Labaume et al. 2016a) controlled the westward progradation of these deposits. Finally, during the late Eocene-early Miocene, the molasse deposits of the Campodarbe Group represent the overfilled sedimentation stage of the basin (Puigdefàbregas 1975; Labaume et al. 1985; Oliva-Urcia et al. 2016; Roigé et al. 2019). The central part of the basin (Guarga syncline, Fig. 1B), where the Campodarbe Group reaches more than 3000 m in thickness, is characterized by the interplay of an east-derived fluvial system with a north-derived alluvial-fan system (Puigdefàbregas 1975; Montes and Colombo 1996; Roigé 2018). Four different north-derived alluvial fans can be identified in the Jaca basin: the Santa Orosia, Canciás, Peña Oroel, and San Juan de la Peña fans. The continentalization of the basin was diachronous, from east to west (Puigdefàbregas 1975; Dreyer et al. 1999), and ended at 36 Ma with the closure of the basin and the development of endorheic conditions (Ortí et al. 1986; Payros et al. 1999; Barnolas and Gil-Peña 2001; Costa et al. 2010).

Petrography and Provenance

Roigé (2018) defined the paleogeographic evolution of the Jaca basin drainages describing the interplay between axially fed sediments from the east with transversely fed sediments from the north in the Jaca basin. Four different petrofacies were identified and mapped based on the relative abundance of the most significant components such as hybrid sandstone rock fragments (which are those displaying intrabasinal and extrabasinal grains), feldspar and lithic grains, and carbonate extrabasinal particles.

The "hybrid-clast-dominated" petrofacies (HCD) is characterized by high percentages of hybrid sandstone and/or siltstone rock fragments together with limestone rock fragments, and a low abundance of metamorphic and sandstone rock fragments (Roigé et al. 2017). The "carbonate extrabasinal enriched" petrofacies (CEE) is dominated by carbonate extrabasinal components, subordinate hybrid sandstone rock fragments, and a very low siliciclastic content. In the "siliciclastic dominant" petrofacies (SD), carbonate grains and hybrid sandstone rock fragments are scarce, and shales, schists, and quartzites are the most representative particles, with sandstone and siltstone rock fragments, micas, and feldspar as subordinate grains. The "mixed lithic and carbonate" petrofacies (MLC) displays a high percentages of carbonate grains, hybrid sandstone rock fragments and lithic grains.

During the deposition of the Banastón turbidite system of the upper Hecho Group (Fig. 2), "carbonate extrabasinal enriched" sediment entered the basin sourced from the east (east-central Pyrennees). During the deposition of the overlying Jaca turbidite system, this eastern source evolved to a more siliciclastic composition (Roigé et al. 2017). The last turbidite sedimentation stage (the Rapitán channel) displays the first composition derived from northern sources (HCD petrofacies), evidenced by the increase in sandstone rock fragments. In the Bartonian-Priabonian, deltaic environments record the strong interplay between the axially fed "carbonate enriched" and "siliciclastic dominant" sediments with the first transverse alluvial fans characterized by the abundance of hybrid sandstone rock fragments that can be linked to the uplift and recycling of the former turbidite basin. The interplay between these two drainage patterns is further evidenced by the occurrence of the "mixed lithic and carbonate" petrofacies in the Peña Oroel and San Juan de la Peña areas, as well as the occurrence of the "hybrid-clast-dominated" petrofacies (Roigé et al. 2017) in the southern flank of the Yebra anticline during the sedimentation of the

Belsué-Atarés delta. Finally, the upper parts of the Canciás and San Juan de la Peña fans also record a compositional evolution highlighted by the increase of lithic and carbonate grains.

Potential Sources of Heavy Minerals

The ability of source to produce a rich and varied heavy-mineral suite depends on the rock type (Mange and Maurer 1992; Garzanti and Andò 2007a, 2007b). Igneous and metamorphic rocks may contain various heavy minerals as the main constituents or accessory phases. By contrast, the heavy-mineral content of sedimentary rocks does not exceed 1% of the total volume. Usually, sandstones may be able to produce a recycled ultrastable suite, whereas carbonate rocks are usually devoid of heavy minerals or display very low content, mostly related to aeolian input or diluted suspended material from terrestrial sources.

Potential sources of heavy minerals during the late Eocene-Miocene in the Jaca basin can be: (i) the Paleozoic basement occurring in the Axial or North Pyrenean Zone, (ii) the preorogenic Mesozoic cover successions of the North and South Pyrenean Zone, and (iii) the synorogenic assemblage of late Cretaceous-middle Eocene deposits. The Paleozoic basement is constituted by an assemblage of Cambro-Ordovician to Devonian metasedimentary units, followed by Carboniferous flysch deposits, which are in turn intruded by Variscan granitoids (Carboniferous-Permian) (Zwart and Sitter 1979; Zwart 1986; Debon et al. 1996 Guitard et al. 1996; Ribeiro et al. 2019). In general, the whole Paleozoic basement displays a very-low to low grade of metamorphism, though it increases to medium and high grade in large metamorphic domes that occur along the the Axial Zone.

The Paleozoic basement of the Pyrenees is unconformably overlain by Permo-Triassic red beds or Cretaceous limestones. Shales, carbonates (Muschelkalk facies), evaporites (Keuper facies), and dolerites (ophites) complete the Triassic succession. The Jurassic and Cretaceous in the Southern Pyrenees are mainly represented by a thick carbonate and shale succession. Nonetheless, in the North Pyrenean Zone, (Fig. 1) a Jurassic-lower Cretaceous carbonate succession is followed by a thick sequence of deep-water shales and turbidites (Albian to Maastrichtian) intruded by subvolcanic basaltic rocks (Souquet 1967; Azambre 1967). A Cretaceous HT-LP metamorphism appears restricted to a narrow east-west-trending belt (Internal Metamorphic Zone) in the North Pyrenean Zone, related to crustal thinning and mantle exhumation during the rifting (Goldberg and Leyreloup 1990, Clerc et al. 2015). Subsequent foreland-basin deposits are best preserved in the Southern Pyrenees Platform carbonates (limestone, dolostone, and sandstone deposits) developed in the distal basin margin from Cretaceous to Lutetian times whereas the basin trough was characterized by the Eocene clastic infill of the Àger, Tremp, Ainsa, and Jaca basins, which mainly consist of siliciclastic alluvial, deltaic, and turbidite deposits.

Zircon, tourmaline, rutile, and apatite grains occur in a wide variety of igneous, sedimentary, and metamorphic rocks of the Paleozoic basement, Mesozoic metamorphic rocks, and Mesozoic and Tertiary sedimentary cover (Fig. 3). Minerals such as chloritoid, almandine, staurolite, and kyanite are prone to be derived from Paleozoic metapelites (phyllites, schists, and granulites; Zwart and Sitter 1979; Zwart 1986; Guitard et al. 1996) but have not been reported in the Mesozoic metapelites of the Internal Metamorphic Zone. Almandine garnet might be also sourced from igneous rocks such as Permo-Carboniferous rhyolites, dacites, ignimibrites, and volcaniclastic sediments (Bixel 1987; Gilbert and Rogers 1989) or late Variscan muscovite granites (Harris 1974). By contrast, grossular garnet is usually associated with skarn deposits, thermally metamorphosed impure limestones and marbles occurring in the Axial and North Pyrenean zones. In addition, grossular has also been described in volcanic rocks such as the syenites of the North Pyrenean Zone (Azambre et al. 1989).

Clinopyroxene, olivine, spinel, epidote, and amphibole occur in various igneous rocks such as Triassic dolerites or Cretaceous basalts, picrites, teschenites, syenites, and lamprophyres of the North Pyrenean Zone (Azambre 1967; Azambre et al. 1987, 1989; Ternet et al. 1995; Lago et al., 2000). Clinopyroxene and amphibole are also common in basic igneous rocks (basalts and andesites) of the Stephano-Permian vulcanism (Bixel 1987). In addition, epidote, amphibole, clinopyroxene, titanite, and vesuvianite also occur in Paleozoic marbles and calcschists, skarn deposits, and hornfels related to Paleozoic granites, as well as in the metamorphic Mesozoic limestones of the North Pyrenean Zone (Ternet et al. 1995; Majesté-Menjoulàs et al. 1999). Spinel and olivine, as well as clinopyroxene and amphibole, are also present in regionally metamorphosed carbonate rocks that have achieved the amphibolite facies. Titanite is common accessory mineral in many igneous and metamorphic rocks, and thus it can be found in Paleozoic granites, Triassic dolerites, metapelites, and impure calc-silicate rocks (Azambre 1967; Azambre el al. 1987; Zwart and Sitter 1979; Zwart 1986; Guitard et al. 1996; Ribeiro et al. 2019).

SAMPLING AND METHODS

A total of 24 samples of sandstone were collected from five sections (Jaca, Santa Orosia, Canciás, Peña Oroel, and San Juan de la Peña) for heavy-mineral analysis of the turbidite, deltaic, and fluvio-alluvial deposits of the Jaca basin. In cases where medium-grained sandstone was not available, fine to very coarse grain sizes were collected. In addition, samples from each depositional system were collected from similar facies in order to minimize hydraulic-sorting effects related to different processes within the same depositional environment (Andò et al. 2019). They were crushed and submitted to digestion with diluted 10% acetic acid for carbonate removal and better desegregation of well cemented sands. The 32 to 500 µm window was recovered through wet sieving prior to heavy-mineral separation. The heavy fraction was separated by centrifuging in Na-polytungstate (2.90 g/cm^3) and recovered by partial freezing with liquid nitrogen (e.g., Mange and Maurer 1992, Andó 2020).

Polished thin sections (30 micrometers) of the heavy-mineral fraction were prepared for each sample, and mineral identification was done using Raman spectroscopy. The counting method used was the ribbon or area method (Galehouse 1971). A representative area of the thin section was selected, and all the minerals in that area up to 200 grains were identified. The obtained Raman spectra (Figs. 4, 5) were compared with reference spectra (Wang et al. 2004; Kuebler et al. 2006; Andò and Garzanti 2014) and verified under the optical microscope. Opaque, diagenetic, carbonate, and micaceous minerals were not considered for identification, and only the relative abundances of detrital heavy minerals are reported in this paper. Statistical treatment of the heavy-mineral counting data was done using the Provenance R-package (Vermeesch et al. 2016; Vermeesch 2018). In addition, heavy-mineral analysis was integrated with sandstone petrography data already published in Roigé (2018).

Since the data obtained by the area method are counts, correspondence analysis with the provenance R package (Vermesch 1018) was used for the statistical treatment. This procedure may introduce some bias as point-counting was not the method used to acquire the data. However, in multi-dimensional datasets, this is a good way to visualise and interpret the results of counts.

RESULTS

The relative abundances of heavy minerals (Tab. 1) of the study samples are presented as percentage pie charts in their stratigraphic position (Fig. 6) for optimal visualization and integration with sandstone petrography (Roigé et al. 2016, 2017). Since all samples display more than 71.1% of the ultrastable association Ap-Zrn-Tur-Rt, the modal relative compositions of each system are presented as Ap (apatite), ZTR (zircon-tourmaline-rutile), and &tHM (other transparent heavy minerals).

The Hecho Group turbidites (91-100% ZTR+Ap) and the Sabiñanigo delta sandstones (96-97% ZTR+Ap) display the higher percentages of the ultrastable suite. Although this assemblage also dominates the alluvial-fan deposits, a clear difference can be observed between the heavy-mineral suites of the deep-marine and the terrestrial environments, since the latter often show higher relative abundances of other transparent heavy minerals (staurolite, garnet, kyanite, chloritoid, titanite, epidote, clinopyroxene, amphibole, vesuvianite, spinel, olivine, or sphalerite) and an increase of the ultrastable ZTR. Moreover, the turbidite deposits are dominated by euhedral, angular and subrounded grains (Ap-Zrn-Tur-Rt), whereas the alluvial-sedimentation stage records an increase in rounded to well-rounded grains.

Jaca Profile

This profile addresses the heavy-mineral suites of the Hecho Group turbidites. The Banastón turbidite system (CEE petrofacies) is dominated by zircon, tourmaline, and rutile (Ap_{41}-ZTR_{57}-&tHM_{2}), whereas the Jaca turbidite system (Ap_{58}-ZTR_{37}-&tHM_{5}) and the Rapitán channel (HCD petrofacies, Ap_{58}-ZTR_{33}-&tHM_{9}) contain the highest relative abundances of apatite. Nonetheless, the lower part of the Jaca turbidite system is similar to the Banastón turbidite system regarding their heavy-mineral suites and sandstone composition. The highest apatite content (75.8%) is found in the upper part of the Jaca turbidite system (J9, SD petrofacies). In addition, the Rapitán channel records an increase in other transparent heavy minerals such as almandine, and the first appearance of grossular, clinopyroxene, sphalerite, and staurolite, whereas the former turbiditic systems area characterized by the presence of almandine and spinel and chloritoid.

Santa Orosia Profile

This profile starts with the deltaic deposits of the Sabiñanigo sandstone (Ap_{46}-ZTR_{51}-&tHM_{3}), which display a suite similar to that of the Banastón turbidite system, though the relative abundance of apatite in the lower part (55.2%, CEE petrofacies) is much higher than in the upper part (37.1%, HCD petrofacies). Conversely, ZTR increases to the top, from 42% to 59%. As in the Banastón and Jaca turbidites, spinel and almandine are also present in the assemblage.

Upsection, the younger Belsué-Atarés deltaic sandstones (CEE petrofacies) display a different assemblage (Ap_{25}-ZTR_{57}-&tHM$_{18}$) from the Sabiñanigo delta sandstone. As for the Sabiñanigo sandstone, apatite relative abundances are higher at the base (31.2%) than at the top (18.5%), and ZTR increases to the top, from 40% to 74%. However, a characteristic feature of this Formation is the relative abundance of &tHM ($Ttn_{23.9}$-$St_{1.3}$-$Alm_{1.3}$-$Cld_{0.3}$-$Ep_{0.3}$-$Fo_{0.3}$), which in the lower part achieves 29%. By contrast, the upper part displays titanite, staurolite, and almandine as well, but their relative abundances are much lower ($Ttn_{1.3}$-$St_{1.8}$-$Alm_{2.6}$) and there is no trace of epidote, forsterite, or chloritoid.

The overlying deposits of the late Eocene Santa Orosia fan (HCD petrofacies) are dominated by zircon, tourmaline, and rutile (Ap_{30}-ZTR_{53}-$OtHM_{17}$). However, there is a marked increase in other transparent heavy minerals (up to 24% in the middle part of the fan) compared to the former turbidite and delta systems. Titanite, almandine, and staurolite are common, though in low relative proportions ($Ttn_{5.1}$-$Alm_{4.4}$-$St_{4.4}$). A characteristic feature of the Santa Orosia alluvial fan is the presence of clinopyroxene (0.8%), though it disappears at the top.

Cancías Profile

Here, the Belsué-Atarés deltaic sandstones (Ap_{44}-ZTR_{54}-$OtHM_{2}$) display higher relative abundances of apatite and less of other transparent heavy minerals ($Alm_{1.4}$-$Grs_{0.5}$-$Ep_{0.5}$) compared to the Santa Orosia profile. The overlying Oligocene Canciás fan displays a different assemblage (Ap_{30}-ZTR_{70}-&tHM$_{16}$), highlighted by the increase in other transparent heavy minerals. It is important to notice that this fan records three different compositions trough the "hybrid-clast-dominated", "mixed lithic and carbonate", and "carbonate enriched" petrofacies. In the lower part (C8, Ap_{29}-ZTR_{59}-&tHM$_{13}$), the assemblage is similar to the one occurring at the top of the Sta. Orosia fan (JY39, Ap_{31}-ZTR_{55}-&tHM$_{14}$), with similar relative proportions of almandine, staurolite, titanite, and grossular (C8, $Alm_{3.9}$-$St_{4.4}$-Ttn_{2}-$Grs_{0.5}$; JY39, $Alm_{4.3}$-$St_{3.1}$-$Ttn_{3.5}$-$Grs_{1.2}$), and both corresponding to the "hybrid-clast-dominated" petrofacies. Up section, sample C13 (Ap_{0}-ZTR_{85}-&tHM$_{14}$, MLC) is characterized by the scarcity of apatite (0.5%) and the high content of tourmaline (62.7%). In the "hybrid-clast-dominated" upper part of the fan (C17, Ap_{13}-ZTR_{66}-&tHM$_{21}$) the heavy-mineral suite records an increase in the epidote relative abundance (14.2%) as well as apatite (13%), though its content is low compared to the lower part of the fan. Another interesting feature is that grossular dominates over almandine in the upper part of the Canciás fan, whereas in the lower turbiditic, deltaic, and alluvial deposits (Sta. Orosia and lower Canciás fan) almandine is more abundant than grossular. Staurolite is also less common in the upper part (0.5%) of the Canciás fan than in its lower part (4.4%) or the Sta. Orosia fan (4.4%).

Peña Oroel Profile

Here, the Belsué-Atarés Formation (Ap_{12}-ZTR_{66}-&tHM_{22}) displays the highest relative abundance of other transparent heavy minerals in two different petrofacies (HCD petrofacies, Ap_{12}-ZTR_{61}-$OtHM_{27}$; MLC, Ap_{12}-ZTR_{71}-&tHM_{17}). The most characteristic feature of these suites is the presence of clinopyroxene and vesuvianite, especially in the lower "hybrid-clast-dominated" part (Cpx, 12.6%; Ves, 2.3%). Both petrofacies show a similar heavy-mineral assemblage, though sample JJ6 (MLC petrofacies) does not record the presence of vesuvianite, the clinopyroxene relative abundance is lower (3.1%), and zircon increases up to 34.4%.

The characteristic feature of the Peña Oroel fan is the predominance of the "hybrid-clast-dominated" petrofacies through the entire section. Similar to the Canciás profile, these alluvial deposits (Ap_8-ZTR_{72}-&tHM_{19}) exhibit low relative abundances of apatite, high ZTR, and higher content of other transparent heavy minerals when compared to the Hecho turbidite deposits. As in the Santa Orosia fan, in the Peña Oroel alluvial deposits the most abundant garnet is almandine (6%), and staurolite is common (5%). The upper part of the fan records the occurrence of kyanite, actinolite, clinopyroxene, and vesuvianite.

San Juan de la Peña Profile

This profile starts with the fluvial deposits of the Campodarbe Formation. These sandstones are classified as "siliciclastic dominant" petrofacies and their heavy-mineral suite is dominated by apatite (Ap_{40}-ZTR_{33}-&tHM_{27}). However, they show the highest relative abundance of other transparent heavy minerals ($Cld_{9.8}$-$Grs_{5.7}$-$Cpx_{5.2}$-$Ttn_{2.1}$-$Alm_{1.5}$-$Ep_{0.5}$), with chloritoid, grossular, and clinopyroxene being the most represented. Almandine, titanite, and epidote are also present.

By contrast, the overlying late Oligocene to Miocene San Juan de la Peña alluvial-fan system, where the dominant petrofacies is the "hybrid-clast-dominated", exhibits higher relative abundances of ZTR and minor apatite (Ap_{10}-ZTR_{67}-&tHM_{22}). However, this fan records a compositional change in the upper part, where sandstones are classified as "mixed lithic and carbonate" petrofacies. Although epidote is also present in the lower parts of the fan (0.9%), the compositional change is accompanied by an increase of epidote relative abundance (up to 17.5%). Other heavy minerals present in the alluvial sediments are clinopyroxene, titanite, actinolite, almandine, grossular, staurolite, vesuvianite, and spinel.

Statistical Treatment

In the previous section, results were described in terms of the relative abundances of heavy minerals. However, such a display does not consider the statistical uncertainty of the counting data (Vermeesch 2018). The best way to solve this problem in multi-dimensional datasets is to visualize and interpret the results through correspondence analysis (Greenacre 1984). Therefore, a set of biplots are used to visualise the results of the statistical analysis. The first one (Fig. 7A) shows the correspondence analysis of the raw data. Although it does not explain the overall variance in a satisfactory way, it clearly shows a correlation between some minerals. Apatite correlates with chloritoid and sphalerite; spinel with forsterite; zircon with tourmaline and rutile; finally, there is a correlation between the rest of the minerals.

Due to the scarcity of some minerals, zero values dominate the data (Table 1). This might be a problem when applying correspondence analysis because this method is very sensitive to the least abundant components (Vermeesch 2018). In order to avoid undesirable noise, minerals were grouped based on the correlations shown by the correspondence analysis of the raw data. A new analysis was performed (Fig. 7B), accounting for as much as 88.5% of the variance and maintaining the original structure of the biplot.

Figure 7C shows that samples from the turbidite systems cluster around apatite, indicating that they are compositionally similar and enriched in this mineral. Conversely, alluvial-fan deposits group around the OtHM and ZTR. Samples plot close to epidote in the upper parts of the Canciás and San Juan de la Peña fans (C17 and SP14 respectively), indicating a different composition when contrasting to the lower parts of the fans.

Deltaic deposits display the highest dispersion (Fig. 7C). While the heavy-mineral suites of the Sabiñánigo sandstone are similar to the former turbidites, the mineral assemblages of the Belsué-Atarés sandstone vary depending on the stratigraphic profile and the various petrofacies. The mineral suites of the Belsué-Atarés delta are enriched in apatite in the Canciás profile (C2), whereas the abundance of other transparent heavy minerals is higher in the Santa Orosia (JY15, JY21) and Peña Oroel (JJ5, JJ6) sections. The Belsué-Atarés Formation seems to be compositionally similar in the Santa Orosia (JY15, JY21) and

Peña Oroel profiles (JJ5, JJ6), according to the correspondence analysis (Fig. 7B), though it is enriched in OtHM in the Peña Oroel profile.

Regarding the petrographic analysis of bulk sandstone, there is a correlation between the heavy-mineral assemblages and the petrofacies displayed by each sample (Roigé et al. 2017), though the "carbonate enriched" and the "hybrid-clast-dominated" petrofacies show some dispersion (Fig. 7D). The "carbonate enriched" and the "siliciclastic dominant" petrofacies are enriched in apatite, whereas the characteristic feature of the "hybrid-clast-dominated" and the "mixed lithic and carbonatic" petrofacies is their higher relative abundance of other transparent heavy minerals (OtHM) and ZTR.

DISCUSSION

Provenance vs. Diagenetic Overprint

Before attempting to extract any provenance interpretation based on detrital heavy-mineral assemblages of ancient rocks, one has to be aware of the overprinting processes, which can modify the original detrital signature (Morton and Hallsworth 1999; Garzanti et al. 2008, 2009, 2018; Garzanti and Andò 2019). Source-rock lithology exerts the main control on the composition of detrital heavy-mineral assemblages. However, weathering at the source area, physical sorting, and, particularly, dissolution during deep-burial diagenesis can modify the final absolute or relative abundances of heavy minerals found in a detrital rock. Many authors have faced the issue of intrastratal dissolution, a process that can greatly modify the detrital assemblages during deep-burial diagenesis (Morton 1984, Milliken 1990; Morton and Hallsworth 1999, 2007; Velbel 2007; Andò et al. 2012; Garzanti and Andò 2007a, 2019). Substantial loss of heavy minerals has been described in many basins of the world (Walderhaug and Porten 2007; Milliken and Mack 1990; Morton and Hallsworth 2007; Garzanti et al. 2018) with increasing burial depth, but a given mineral may dissolve or remain at different depths in different basins. Nevertheless, there is a consensus in the order of persistence of different heavy minerals with burial. Basically, dissolution depends on pore-fluid temperature and composition, the rate of pore-fluid movement, and geological time (Morton and Hallsworth 2007). The study of dissolution textures (Andò et al. 2012) combined with paleotemperature data and integration of sandstone petrography, can provide some insights about the possible loss of minerals due to deep-burial diagenesis.

In the Jaca basin, the main difference between the heavy-mineral suites of the turbidite and the alluvial sedimentation stages is the increase of unstable heavy minerals displayed by the terrestrial environments. This is a typical pattern when older and more deeply buried sandstones have gone through stronger diagenesis than younger and less deeply buried sediments. Since burial diagenesis may account for the ultrastable assemblage displayed by the turbidite and deltaic deposits, each section is analyzed separately in order to properly assess the degree of diagenetic overprint based on paleotemperature data and dissolution textures.

Jaca Profile.---In this profile, the ultrastable association of the Hecho Group turbidites might be the result of intrastratal dissolution due to burial depth. However, erosion of felsic acidic igneous rocks or ancient sandstones may produce a similar suite (Götze 1998). Based on the high content of terrigenous carbonate grains, feldspar, and plutonic rock fragments, Roigé et al. (2016) established that the Banastón and the lower Jaca turbidite systems were sourced mainly from the Mesozoic and Paleocene platform carbonates of the South-Central Pyrenean Unit and granitoids of the Paleozoic basement (east-central Pyrenees). As carbonate rocks are poor "heavy-mineral suppliers", it is more likely that the assemblage was derived mainly from the erosion of granitic sources, especially those grains that display a euhedral to angular character, which are more abundant in the Banastón and lower Jaca turbidite system. Conversely, the more rounded grains might be sourced from the recycling of the Paleocene or Cretaceous sandstone formations, which is in accordance with the occurrence of well-rounded quartz grains recorded by sandstone petrography (Roigé et al. 2017). In addition, the occurrence of siliciclastic sandstone rock fragments and detrital quartz grains with inherited overgrowths, together with early Variscan detrital zircon U-Pb dates (Roigé 2018), points to the Carborniferous flysch as another possible source for the more rounded heavy-mineral grains.

The observation of dissolution textures on grains provides important insights into the possible loss of minerals due to deep-burial diagenesis or weathering processes. Ultrastable minerals (Ap-Zrn-Tur-Rt), display unweathered or only initial corrosion features (Fig. 8). Almandine also show no signs of corrosion, although in the lower part of the Jaca Turbidite system some grains display advanced corrosion features (Fig. 8) pointing to a higher impact of diagenesis, probably more intense in the Banastón turbidite system.

By contrast, the occurrence of uncorroded clinopyroxene (1.3%) in the Rapitán channel just 700 m above the top of the Banastón turbidite system might indicate that dissolution processes were not too intense, at least in the Jaca turbidite system. Clinopyroxene is well known for its instability during deep burial, only more resistant than olivine (Morton 1984; Morton and Hallsworth 1999, 2007), therefore being a good proxy to assess diagenesis importance. These clinopyroxene grains, as well as almandine and grossular (Fig. 8), display incipient degree of corrosion (Andò et al. 2012) (Fig 8), pointing to a low impact of diagenesis on the heavy-mineral suites. Since no etched or skeletal clinopyroxene grains have been reported, we infer that dissolution processes due to intrastratal dissolution probably were not too intense. Therefore, we infer that if unstable minerals dominated the original assemblage of the Jaca turbidites, the 700 m depth difference between the Rapitán Channel and the lower Jaca turbidite system does not seem to be enough to completely erase more stable minerals such as epidote, titanite, kyanite, staurolite, or garnet from the sedimentary record since clinopyroxene is well known for its instability during deep burial, only more resistant than olivine (Morton 1984; Morton and Hallsworth 1999, 2007). Moreover, in the Norwegian continental shelf, ultrastable zircon, tourmaline, rutile, apatite, and spinel exceed depths of 5000 m and more than 200ºC without dissolution features. Epidote is able to survive burial temperatures up to 95ºC, whereas staurolite and garnet can survive up to 110ºC and 175ºC respectively (Walderhaug and Porten, 2007). Thermal modelling of the Jaca basin (Crognier 2016) and apatite fission-track data (Labaume et al. 2016a) revealed that maximum paleotemperatures for the upper Hecho Group turbidites remained below 90ºC in the Jaca section (70ºC according to vitrinite reflectance). Therefore, the absence of these minerals or at least the low abundance of garnet and staurolite is most likely a provenance effect rather than a diagenetic feature, though loss of minerals due to intrastratal dissolution cannot be completely discarded as evidenced by some advanced corrosion features in almandine grains (Fig. 8). Nonetheless, the heavy-mineral assemblages of the Banastón and the Jaca turbidite systems are coherent with the erosion of granitic sources, ancient sandstones, and very low- to low-grade metamorphic terrains.

Santa Orosia Profile.---According to thermal modelling (Crognier 2016), the 90ºC paleotemperature isotherm should be at aproximately 2500 m below the top of the Santa Orosia fan. Therefore, maximum paleotemperatures for the Sabiñanigo and the Belsué-Atarés formations in the present-day outcrops would be 75ºC and 50ºC respectively, according to sediment thickness. In fact, vitrinite-reflectance measurements in the northern flank of the Yebra anticline indicate a maximum paleotemperature of less than 60ºC for the Sabiñanigo sandstone (Labaume et al 2016). Therefore, minerals such as epidote, staurolite, or garnet would have survived these temperatures, at least without advanced dissolution features. This is the case for garnet (almandine and grossular) and staurolite, in that the grains present in the Sabiñanigo sandstone show only unweathered or initially corroed surface textures (Fig 9), thus suggesting that they were not significantly affected by intrastratal dissolution. Moreover, olivine grains (the most unstable mineral under burial diagenesis) in the Belsué-Atarés delta, as well as in the Santa Orosia alluvial fan, also show unweathered or initially corroed surface textures (Fig 9). Therefore, their relative abundance seems to be a provenance signal, as well as the high relative abundance of the ultrastable suite Ap-Zrn-Tur-Rt and the absence of epidote.

Upwards in the section, the lower part of the Belsué-Atarés Formation displays a sudden input of titanite and records the presence of almandine, staurolite, chloritoid, epidote, and forsterite (the latter known as the most unstable heavy mineral; Morton and Hallsworth 1999), whereas the upper part shows a strong decrease in titanite together with the absence of chloritoid, epidote, and forsterite (Table 1, Fig. 6). Here, the low abundance of unstable minerals seems to be a provenance feature of the Belsué-Atarés Formation, since burial temperatures should be lower than in the Sabiñanigo sandstone. These deltaic deposits are characterized by the "carbonate extrabasinal enriched" petrofacies, where detrital carbonates are the most abundant component (Roigé et al. 2017). Nevertheless, the siliciclastic population contains volcanic and metamorphic rock fragments (phyllites, schists, chloritoschists, and quartzites) that are problably linked to the occurrence of almandine, staurolite, chloritoid, titanite, and epidote. Almandine, staurolite, and chloritoid are prone to be sourced from phyllites and schists, whereas forsterite is more likely to be derived from basic igneous rocks, although it could be sourced from dolomitic marbles as well. Titanite and epidote could be linked to both types of rocks.

Anomalous high paleotemperatures were detected in the northern flank of the Canciás syncline, close to the Oturia thrust, related to fluid flow along the fault (Labaume et al 2016). However, it is probable that maximum paleotemperatures achieved by the Santa Orosia fan were much lower in the southern flank of the Canciás syncline. Occurrence of fresh clinopyroxene in the lower part of the Santa Orosia fan may indicate that loss of unstable minerals in this area is not significant and supports the idea of low paleotemperatures in the southern part of the Santa Orosia fan.

The Santa Orosia alluvial-fan deposits are characterized by the "hybrid-clast-dominated" petrofacies, where recycled turbidite rock fragments are the most abundant component. Therefore, part of the Ap-Zrn-Tur-Rt assemblage is probably a consequence of the recycling of the older turbidite basin, in as much as the characteristic feature of the Hecho Group turbidites is a high content of Ap-Zrn-Tur-Rt.

Even other minerals, such as garnet or staurolite, might be able to survive the recycling process and could be linked to the recycling of the former turbidite basin (Mange and Maurer 1992). However, the fact that staurolite has been reported only in the Rapitán channel (1%), and titanite is absent in all the turbidite systems but present in the St. Orosia fan, suggests that additional metamorphic and/or igneous sources were the main suppliers of these minerals. Authigenic titanites have been described in the literature. However, since they display mainly angular to subrounded textures they have been interpreted as detrital, also excluding the possibility of recycled old authigenic titanite since no rounded to well-rounded titanites have been obserbed. Moreover, the occurrence of metamorphic and volcanic grains in the sand fraction of the alluvial-fan deposits supports the idea of staurolite and titanite being supplied from a direct source rather than a recycled origin and reinforces the idea that igneous and metamorphic sources also contributed to the Ap-Zrn-Tur-Rt suite.

Canciás Profile.---In the lower part of this profile, the Belsué-Atarés Formation records the presence of epidote and very low proportions of almandine and grossular (Table 1, Fig. 6). Paleotemperatures in the present-day outcrops of this profile remained below 90ºC (Crognier 2016). Thus, the low proportion of garnet appears to be a provenance signal rather than a diagenetic overprint. This also seems to be the case for epidote, though it is less stable than garnet and its scarcity could be related to burial diagenesis. Nonetheless, the absence of titanite and staurolite, both more stable than epidote but less than garnet, do seem to mirror its absence in the source area.

In the upper part of the section, titanite, staurolite, almandine, grossular, and epidote are present in the Canciás fan deposits (Table 1, Fig. 6). As in the Santa Orosia fan, the presence of these minerals points to the erosion of new source areas consisting of metamorphic and igneous rocks. Almandine and staurolite are probably related to the erosion of the Paleozoic basement, whereas titanite could also be sourced from Triassic and Cretaceous igneous rocks. However, sandstone petrography does not record the occurrence of volcanic rock fragments in the lower and middle Canciás fan. By contrast, phyllites, schists, and quartzites do occur, and therefore the source of titanite is more likely to be metamorphic than igneous. Grossular could be derived from thermally metamorphosed limestones occurring in the Paleozoic basement, as well as in the North Pyrenean Mesozoic, or even from syenites occurring in the North Pyrenean Zone. Nonetheless, no evidence of these rock types is found in the sand fraction of the alluvial deposits. Epidote is probably linked to the erosion of basic igneous rocks, such as Triassic dolerites, that have undergone spilitization. Occurrence of volcanic clasts in the upper part of the fan clearly supports this origin (Roigé et al. 2017).

The middle Canciás fan records an extreme low relative abundance of apatite, which contrasts with the Santa Orosia alluvial fan and the lower part of the Canciás fan. Both fans record the recycling of the Hecho Group turbidites, where apatite is the most abundant mineral. However, whereas the younger Santa Orosia fan displays high abundances of apatite, this mineral is almost absent in the Canciás fan. Furthemore, apatite it is present in all samples, and its absence is not a characteristic feature of the mixed lithic and carbonate petrofacies, as evidenced by its occurrence in the Peña Oroel and San Juan de la Peña sections. Since some advanced dissolution textures displayed by apatite and tourmaline grains (Fig. 10) suggesting weathering processes, we infer that periods of acidic groundwater percolation (Morton and Hallsworth 1999) in the present-day outcrops, alluvial storage, or most likely weathering at the source area might account for its almost complete absence, since apatite is the most unstable mineral under weathering conditions (Morton and Hallsworth 1999).

According to paleotemperature distribution in the area (Crognier 2016), it is very unlikely that the upper part of the Canciás fan was deeply buried. Therefore, the sudden increase of the epidote relative abundance, just below the compositional change from the "hybrid-clast-dominated" to the "carbonate extrabasinal enriched" petrofacies, is probably related with this compositional change rather than to dissolution processes. Furthermore, it implies that the lower part of the fan probably displays its detrital provenance signature.

Peña Oroel Profile.---In this area, the most characteristic feature of the Belsué-Atarés delta Formation is the abundance of fresh clinopyroxene (12%, Fig. 6). Hence, we infer that the high abundance of this unstable mineral, the fact that no highly corroded or skeletal grains have been observed (Fig. 11 A, B), and that staurolite, grossular, and almandine do not display corrosion features (Fig. 11 C, D, E), indicates that burial diagenesis did not have a profound effect in this area. This is in accordance with paleotemperatures deduced from thermal modelling (Crognier 2016), revealing that the maximum temperature remained below 50ºC.

Here, the Belsué-Atarés delta exhibits the north-derived "hybrid-clast-dominated" petrofacies, though to the top, a compositional change is observed due to the interaction with the east-derived "siliciclastic dominant" input. Due to this mixing, the upper deltaic deposits display the "mixed lithic and carbonate" petrofacies. However, samples from both petrofacies plot close (Fig. 7D), highlighting their compositional similarity regarding their heavy-mineral signature. The fact that the siliciclastic content of both petrofacies is probably the main source of heavy minerals might be the reason why the heavy-mineral provenance signatures of both petrofacies do not show significant differences. The presence of vesuvianite and grossular as well as clinopyroxene point to a source consisting of impure limestones that have gone through thermal metamorphism, though clinopyroxene could also be sourced from basic igneous rocks. Occurrence of paleovolcanic lithic rock fragments with lathwork texture made of plagioclase and altered augite in the Belsué-Atarés Formation (Roigé et al. 2017) points to an igneous origin for clinopyroxene. Therefore, vesuvianite and grossular most probably derive from the thermally metamorphosed Mesozoic limestone hosts of these volcanic rocks.

In the Peña Oroel alluvial fan, occurrence of almandine, staurolite, and even kyanite points to erosion of the Paleozoic metapelites, although they could have a recycled origin from Cretaceous sandstones as the Marboré Sandstone (Recio et al. 1987). The Ap-ZTR ultrastable suite could also be derived from the recycling of the turbidite basin, erosion of igneous and metamorphic sources, or Mesozoic and Paleocene sandstones.

San Juan de la Peña Profile.---In the San Juan de la Peña profile, the fluvial Campodarbe Formation also displays uncorroed (Fig. 11F) or slightly corroded (5.1%, Table 1, Fig. 6) clinopyroxene. From this data, we infer that although diagenesis could reduce the total original amount of heavy minerals present in the sediments, no extensive dissolution of heavy minerals seems to have occurred. If other unstable minerals such as Epidote (more unstable and common than clinopyroxene in the Pyrenean context) would have occurred in proportions similar to that of clinopyroxene, dissolution in this profile would have not been enough to completely erase Ep from the sedimentary record.

The statistical analysis (Fig. 7D) reflects three different heavy-mineral assemblages that coincide with the three different petrofacies. The "siliciclastic dominant" petrofacies displayed by the fluvial Campodarbe Formation is enriched in apatite. The "hybrid-clast-dominated" petrofacies is characterized by higher relative abundances of other transparent heavy minerals and ZTR. Finally, the characteristic feature of the "mixed lithic and carbonate" petrofacies is its high relative abundance of epidote (18%).

As for the former alluvial fans, the origin of the Ap-ZTR assemblage can be attributed to recycling of the turbidite basin, or from Paleozoic, Paleocene, and Mesozoic sandstone sources, or directly sourced from igneous and metamorphic rocks. The presence of staurolite, almandine, and chloritoid points unequivocally to metamorphic sources of the Paleozoic basement, whereas clinopyroxene, epidote, actinolite, titanite, vesuvianite, and grossular could be also sourced from Mesozoic subvolcanic rocks and their thermally metamorphosed hosts. Occurrence of volcanic rock fragments in the fluvial Campodarbe Formation is probably related to the presence of clinopyroxene, titanite, and epidote. Conversely, its high relative abundance of chloritoid, an abundant mineral in Carboniferous slates (Zwart 1986), must be linked to the high abundance of metamorphic rock fragments sourced from the Paleozoic basement.

In the San Juan de la Peña fan staurolite, almandine, and even kyanite also point to metamorphic sources of the Paleozoic basement, whereas clinopyroxene, epidote, actinolite, and titanite are most likely to be derived from Triassic or Cretaceous igneous rocks, as evidenced by the presence of volcanic rock fragments in the sandy fraction. Vesuvianite and grossular reinforce this idea, since they would be derived from the thermally metamorphosed limestones that host the igneous rocks.

General Remarks.---According to our results, the Hecho Group turbidites display an ultrastable heavy-mineral suite. By contrast, the alluvial deposits show a more varied assemblage with highly unstable minerals such as clinopyroxene, indicating that intrastratal dissolution did not play a critical role. From the ultrastable suite displayed by the Hecho Group turbidites we cannot exclude a possible diagenetic overprint on their original detrital assemblages. Controversially, our results differ largely from Valloni et al. (1984) who reported a very unstable heavy-mineral suite, characterized by high abundance of augite and garnet but no apatite in the Jaca-Fiscal turbidites. However, our data show that apatite is a characteristic mineral of the upper Hecho Group turbidites, garnet relative abundance is very low, and clinopyroxene is absent in the Banastón and Jaca turbidite systems, being present only in the Rapitán channel (1.3%). Moreover, Valloni et al. (1984) reports the presence of glaucophane and riebeckite in these deep-marine deposits. However, these metamorphic minerals have never been described in the Pyrenees, most likely because they imply a degree of metamorphism (blueschist facies) that was never achieved during the Variscan or Pyrenean orogenic cycles (Zwart and Sitter 1979; Zwart 1986; Guitard et al. 1996; Ribeiro et al. 2019). Since heavy-mineral identification under the microscope in the Hecho Group turbidites could be an arduous task due to the degree of turbid minerals, our use of the more objective Raman spectroscopy technique for mineral identification might account for the differences between our results and those from Valloni et al. (1984).

Therefore, although the Hecho Group turbidites are the formation most affected by burial diagenesis, it seems that the effect of mineral dissolution is not enough to completely erase minerals such as epidote from the detrital record. Moreover, burial diagenesis is slight in the Belsué-Atarés delta (Peña Oroel profile) and the fluvial Campodarbe (San Juan de la Peña profile) formations, and probably plays a minor role in the Sabiñanigo and the Belsué-Atarés deltaic formations in the Santa Orosia profile (Figs. 2, 6), according to paleotemperature distribution and the occurrence of detrital unstable minerals such as olivine.

Although the overlying alluvial fans are also dominated by an ultrastable ZTR heavy-mineral suite, they display a more varied assemblage containing other minerals such as grossular, staurolite, titanite, epidote, and clinopyroxene. These heavy-mineral signatures are similar to the ones recorded by other Pyrenean alluvial fans. For instance, in the Sis fan (Tremp-Graus basin), the Eocene-Oligocene conglomerates (Vincent 2001; Beamud et al. 2003) that record the exhumation of the east-central Pyrenees also display a heavy-mineral suite dominated by ultrastable Ap-Zrn-Tur (Michael 2013). Other transparent heavy minerals are scarce, except for garnet (a common mineral) and epidote. The latter dominates the assemblages in the upper part of the Sis alluvial deposits. Even at the top of the fan, where metasedimentary clasts (phyllites and slates) represent more than the 35% of the clasts, zircon, tourmaline, and apatite are the second most common minerals and there is no trace of other metamorphic minerals such as staurolite, chloritoid, andalusite, sillimanite, or kyanite. This is in accordance with the typical heavy-mineral suites derived from a fold-and-thrust belt, where the sedimentary cover provides few and mainly recycled minerals and only the erosion of the low-medium to high metamorphic and igneous basement would supply minerals such as garnet, staurolite, chloritoid, titanite, clinopyroxene, epidote, or kyanite (Garzanti and Andò 2007b). However, erosion of very low- to low-grade metamorphic rocks and granites can also produce a Tur-Zrn-Rt-Ap dominated heavy-mineral assemblage. Hence, in the Jaca basin, we infer that the detrital heavy-mineral assemblages of all the alluvial fans were not modified in a significant way by intrastratal dissolution, and therefore they display their provenance signature. Moreover, the dominance of the ultrastable suite Ap-Tur-Zrn-Rt in this wedge-top basin seems to reflect the abundance of these minerals in their source rocks rather than a strong diagenetic feature.

The heavy-mineral signatures of the sedimentary infill of the Jaca basin record an increase in the relative abundance of the ultrastable ZTR and other unstable minerals together with a decrease in apatite relative abundance during the alluvial-fan sedimentation stage (Fig. 6; Table 1). This reflects the recycling process of the turbidite basin, since zircon, tourmaline, and rutile are the most resistant minerals to weathering and recycling processes (Mange and Maurer 1992; Garzanti and Andò 2007b; Garzanti et al. 2013a). Moreover, the increase of rounded and well-rounded ZTR grains, when compared to the former turbidite and deltaic deposits, evidences this processes, which is a typical pattern in foreland basins where sediment recycling is the main process controlling the composition of sediments. By contrast, apatite relative abundance is much lower when compared to the Hecho Group turbidites, probably reflecting paleoweathering prior to recycling. Nevertheless, careful investigation of apatite dissolution textures shows no evidence of intense weathering during alluvial-fan sedimentation. Finally, the occurrence of clinopyroxene, epidote, staurolite, grossular, or titanite, and euhedral to angular apatite, zircon, tourmaline, and rutile grains, also points to the contribution of new crystalline sources to the north of the basin. This feature points to the uplift and contribution of new source areas constituted by the Paleozoic basement and the Mesozoic as the source of the more unstable minerals at the same time that the former turbidite basin was being eroded.

Implications for Sediment-Routing Patterns

During the deposition of the Hecho Group turbidites, sediment input was sourced from the east, in the exhumed areas of the central Pyrenees. The increase of apatite through the Banastón and Jaca turbidite systems can be linked to the increase of siliciclastics recorded by sandstone petrography (Roigé et al. 2016), due to the enhanced exhumation in the Axial zone of the central Pyrenees. By contrast, the last turbidite system (Rapitán channel) records the first appearance of minerals such as clinopyroxene, grossular, staurolite, and sphalerite, highlighting a provenance shift related to the erosion of a new source area. This in accordance with a shift in paleocurrent directions, facies, and bulk petrography (Remacha et al. 2005; Roigé et al. 2016). This change has recently been related to the first north-derived sediments entering the basin due to the uplift caused by the Lakora-Eaux-Chaudes thrust system (Roigé et al., 2016; Labaume et al. 2016a). Therefore, we infer that the first occurrence of clinopyroxene, grossular, and staurolite point to new source areas directly to the north of the Jaca basin by this thrust system, which, although active since earlier times (Teixell 1996), did not reach a threshold topography to become a significant source area to the southern foredeep until latest Lutetian times. Clinopyroxene is most likely to be derived from Triassic subvolcanic rocks (ophites), as evidenced by the occurrence of detrital volcanic rock fragments in the Rapitán channel (Roigé et al. 2016), that crop out in the North Pyrenean Zone or close to the limit with the Axial Zone (i.e., the Bedous area). Grossular, instead, points to thermally metamorphosed impure limestones that can be sourced from Paleozoic or Mesozoic carbonate rocks that have been affected by thermal metamorphism. By contrast, staurolite points to medium- and high-grade metapelitic rocks (staurolite-bearing schists) that should be located in the Paleozoic basement of the Axial Zone or in the North Pyrenean Zone (i.e., Lesponne, Chiroulet, or Barousse Massifs).

After the turbidite sedimentation stage, the Sabiñanigo and Belsué-Atarés deltaic sandstones show an interplay between east- and north-derived sources (Roigé et al. 2016, 2017). The different heavy-mineral provenance signatures of the Beslué-Atarés Formation in the Peña Oroel and the Yebra de Basa area do highlight this interplay of sources. In the Yebra de Basa area, the Belsué-Atarés Formation was sourced from the east during the first stages of sedimentation (northern limb of the Yebra de Basa anticline), as evidenced by its ZTR+Ap heavy-mineral suite and its high content of carbonate extrabasinal grains (Roigé 2016, 2017). However, when the delta progradation reached the southern limb of the Yebra de Basa anticline, its composition evolved to hybrid-clast dominated (northern sources, Roigé et al. 2017), evidencing a reorganization of the drainage network due to the activity of the Gavarnie thrust and the uplift and erosion of the former turbidite basin. This is further supported by apatite fission-track thermochronology data (Labaume et al. 2016a) that reveals that the onset of the exhumation of the turbidite basin took place during the Priabonian (35 Ma). To the west, in the Peña Oroel area, the Belsué-Atarés delta records a mixing of northern and eastern sources, highlighted by the occurrence of clinopyroxene, staurolite, titanite, grossular, actinolite, and the "hybrid-clast-dominated" and "mixed lithic and carbonate" petrofacies. The Late Lutetian-Priabonian Escanilla Formation has been proposed as the proximal time equivalent of the Bartonian-Priabonian east-derived Belsué-Atarés delta. However, the heavy-mineral signatures of the Escanilla and the Belsué-Atarés delta formations do not match. The characteristic feature of the Escanilla Formation is its high content of epidote (> 50%, Michael, 2013), which is almost nonexistent in the east-derived Belsué-Atarés Formation (< 0.5%). Thus, according to heavy-mineral provenance signatures, the Escanilla Formation could not have fed the Belsué-Atarés delta in the northern area of the Jaca basin. During the deposition of the Belsué-Atarés Formation, the Oturia thrust and the Yebra de Basa anticline where active (Priabonian-Rupelian, Labaume et al. 2016a). This geotectonic setting would have produced local relief, depocenters, and a reorganization in the drainage network of the basin that would have yielded to the compartmentalization of the basin during the sedimentation of the Belsué-Atarés delta. Thus, the sediments fed from the fluvial Escanilla Formation (Ainsa basin) could not reach the northern part of the basin.

After the deposition of the Belsué-Atarés deltaic sediments, the Priabonian Santa Orosia fan marks the onset of the alluvial sedimentation stage in the basin. The ultrastable association displayed by these alluvial deposits can be linked to the recycling of the proximal, turbidite foreland basin, which was progressively incorporated in the southward-propagating thrust belt. Apatite fission-track thermochronology data and the inferred thermal modelling of the Hecho Group turbidites reveal that their exhumation took place during the Priabonian, related to the Gavarnie thrusting, and continued until the Miocene with the Guarga thrusting (Labaume et al. 2016a). This is further supported by the dominance of hybrid-sandstone rock fragments recorded by sandstone petrography that were interpreted as the result of the uplift of the former turbidite foredeep due to the activity of the Gavarnie thrust (Roigé et al. 2016, 2017; Labaume et al. 2016a). However, the presence of ultrastable idiomorphic grains (Ap, Zrn, Tur, Rt) together with more unstable minerals (St, Alm, Ttn, Cpx, Ep) points to additional metamorphic and/or igneous sources that can be linked to the occurrence of metamorphic rock fragments in the sand fraction.

Another important feature revealed by the heavy-mineral assemblages of the Santa Orosia alluvial fan, is its similarity with the Belsué-Atarés delta suites in the Peña Oroel area. This feature highlights that the Santa Orosia fan sourced the Belsué-Atarés delta in the latter area. Sedimentological data from Boya (2018) indicates that the Belsué-Atarés delta constitutes the distal equivalent deposits of the Santa Orosia fan in the northern flank of the Oroel syncline. Furthermore, sandstone petrography data from Roigé et al. (2017) reveals that these deposits share the same sediment composition, as both formations display the "hybrid-clast-dominated" petrofacies.

To the east of the basin, the younger Canciás alluvial fan shows heavy-mineral suites similar to those of the Santa Orosia fan. However, the upper part of the fan displays a sudden increase of epidote, probably linked a major erosion of Triassic dolerites (ophites) as evidenced by the occurrence of volcanic rock clasts (Roigé et al. 2017). Therefore, the new source area should be located somewhere where Triassic dolerites were cropping out, such as nearby the Cotiella thrust (north of Ainsa; Ríos et al. 1982). This is supported by sandstone petrography, since the increase of Paleogene and Mesozoic limestone grains recorded in the upper part of the fan point to the erosion of new source areas located in the Peña Montañesa or Cotiella thrusts (Roigé et al. 2017).

The interpretation of the heavy-mineral suite of the fluvial Campodarbe Formation in the San Juan de la Peña (western part of the study area) is challenging. The "siliciclastic dominant" petrofacies and main paleocurrent directions towards the west and northwest imply that these deposits were sourced from the east, somewhere in the south-central Pyrenees, and were transported through the alluvial and fluvial systems of the Ainsa basin (Puigdefàbregas 1975; Roigé et al. 2017; Boya 2018). According to similarities in sediment composition, the upper fluvial Escanilla Formation (Bentham et al. 1992) has been proposed as the proximal equivalent of the fluvial Campodarbe Formation at San Juan de la Peña (Roigé et al. 2017). However, the heavy-mineral signatures of the Escanilla and the Campodarbe formations in the San Juan de la Peña section do not match. The characteristic feature of the Escanilla Formation is its high relative abundance of epidote (> 50%; Michael 2013), which is almost non-existent in the east-derived fluvial Campodarbe Formation (0.5%). Even the Chattian-Aquitanian Graus Formation (overlying the Escanilla Formation in the Tremp-Graus basin, Reynolds 1987) displays a heavy-mineral suite dominated by epidote (> 50%; Coll et al. 2019); therefore neither of these formations could be a feeder of the Campodarbe fluvial system in this sector of the basin based on their heavy-mineral provenance signature. However, an important feature of the Campodarbe Formation is that it has different assemblages in the southern margin of the Jaca basin (Coll et al. 2019). For instance, in the southeastern part of the basin the Campodarbe Formation contains high abundance of epidote, thus enabling the Escanilla Formation as a feeder. Conversely, to the west, epidote is absent, requiring a different source. Therefore, we propose that the similarity between the fluvial Campodarbe in the northern (San Juan de la Peña area) and the one recorded in southern part of the basin indicates that an additional routing system entered the basin from the southern margin (i.e., the Arguís area), giving evidence for the interplay between different routing systems during the sedimentation of the Campodarbe Formation. Further research is needed to fully understand the interplay of provenance signals recorded by this formation in the Jaca basin.

Finally, the youngest alluvial deposits in the basin are the Peña Oroel and San Juan de la Peña alluvial fans. Both have similar heavy-mineral suites, indicating very similar source areas. This fact is also revealed by sandstone petrography, since the "hybrid-clast-dominated" petrofacies is the characteristic feature of these deposits. However, the upper part of the San Juan de la Peña fan records an increase of the relative abundance of epidote, coinciding with a petrofacies change in its upper part, as in the Canciás fan. The presence of epidote at San Juan de la Peña, 50 km to the west of Canciás, is interpreted as derived from the erosion of Triassic dolerites that occur to the north of the basin, in the North Pyrenean Zone (Azambre et al. 1987), showing that the source area was large, extending to this area.

Another important fact can be inferred from the appearance of epidote in the Canciás and the San Juan de la Peña fans. In the older late Lutetian-Oligocene Sis alluvial fan of the northern part of the Tremp-Graus basin (Vincent 2001; Beamud et al. 2003), the first appreciable relative abundance of epidote (20%) appears in the Bartonian conglomerates (Michael 2013). However, in the Jaca basin, epidote does not appear in the sedimentary record (15%) until the upper part of the younger Canciás fan (Priabonian) and more to the west it appears in the Miocene upper part of the San Juan de la Peña fan. Hence, the epidote occurrence in the South-Pyrenean basin is diachronous from east to west, and therefore we infer that it is related to the east-west propagation of the Pyrenean thrust deformation and main uplift.

The dominance of the "hybrid-clast-dominated" petrofacies in all the alluvial systems evidences the recycling process of the former turbidite basin. Since the ultrastable Zrn-Tur-Rt-Ap suite dominates both the Hecho Group turbidites and the alluvial systems, we infer that the main source of this assemblage is the recycling of the Hecho Group turbidites. This is supported by thermocronological data from Labaume et al. (2016a) that reveals that exhumation of the Hecho Group turbidites took place in the Jaca basin from the Priabonian due to the activity of the Gavarnie thrust. However, the presence of other minerals such as epidote, clinopyroxene, olivine, titanite, vesuvianite, amphibole, spinel, or sphalerite and idiomorphic zircon, tourmaline, rutile, and apatite in all the alluvial deposits lends support to continued emerging sources to the north of the basin consisting of Mesozoic and Paleozoic igneous and metamorphic terrains of the Axial or North Pyrenean zones. The occurrence of green subvolcanic ophite clasts and volcanic clasts with amygdaloid texture derived from the North Pyrenean Zone in all the alluvial fans (Roigé et al. 2017) most likely links these heavy-mineral suites to the erosion of the North Pyrenean Mesozoic thermally metamorphosed carbonate hosts and associated basic volcanic rocks and their related. Therefore, the source of these heavy minerals implies that the drainage divide of the paleodrainage system was farther to the north in the middle to late Eocene and migrated to the south since then (Roigé et al. 2017). This is further supported by geomorphological data from Babault et al. (2011) and Ortuño and Vilaplanas (2018). The latter authors deduced that the main drainage divide was located in the North Pyrenean Zone (35 km farther to the north than at the present day in the west-central Pyrenees) according to the distribution of remnants of low-relief topography.

Thermochronological data (Jolivet et al. 2007; Meresse 2010; Labaume et al. 2016b; Bosch et al. 2016) show that most of the western Axial Zone could not have acted as a source until at least the middle to late Eocene Oligocene (AFT cooling ages of 20 to 35 My). Conversely, the North Pyrenean Zone experienced cooling since the early Paleogene (Vacherat et al. 2014; Bosch et al. 2016), thus supporting the North Pyrenean Zone as the main source of Mesozoic and Paleozoic grains. However, areas of the Axial Zone of the west-central Pyrenees such as the Lesponne massif, close to the limit with the North Pyrenean Zone, where staurolite- and almandine- bearing schists occur (Pouget 1989), could be exposed and thus act as a source area already during the late Eocene. Metamorphic rock fragments (schists, phyllites, chloritoschists lithic and quartzites) reported by sandstone petrography in all fans point to a direct Variscan metapelite source for staurolite and almandine that could not be sourced from Mesozoic metacarbonates or igneous rocks. Thermochronological data from apatite fission-track dating (Morris et al. 1998; Jolivet et al. 2007), suggest that areas in the northeastern part of the western Axial Zone were undergoing exhumation at that time. Hence, the heavy-mineral provenance signature of the alluvial fans of the Jaca basin reinforce the idea that during the late Eocene the drainage divide of the transverse drainage system extended to the North Pyrenean Zone, and some local areas of the Axial Zone basement could have been providing sediment as well.

CONCLUSIONS

The heavy-mineral suites of the clastic systems of the northern Jaca basin are dominated by the ultrastable association apatite, zircon, tourmaline, and rutile. The relative abundance of these minerals is higher in the early foredeep turbidite deposits, whereas the characteristic feature of the subsequent alluvial-sedimentation stage is the higher relative abundance of other more unstable heavy minerals such as staurolite, almandine, clinopyroxene, grossular, vesuvianite, titanite, and epidote and an increase of the ultrastable zircon, tourmaline, and rutile assemblage. The heavy-mineral suites of the bulk of the Eocene Hecho Group turbidites can be related to eastern source areas located in the east-central Pyrenees (Axial Zone), shifting to north-derived in the uppermost (late Lutetian) part of the group (North Pyrenean sources). On the other hand, the subsequent alluvial assemblages of the Jaca basin are sourced mainly from the recycling of the earlier turbidite basin, although with contributions from the North Pyrenean deformed belt.

The diagenetic overprint experienced by the Hecho Group turbidites does not seem enough to completely erase minerals such as epidote, titanite, staurolite, or grossular from the sedimentary record or to account for the low abundance of almandine. Furthermore, it seems to be negligible or slight in the overlying deltaic, fluvial, and alluvial environments, at least in the Peña Oroel and San Juan de la Peña areas, where fresh clinopyroxene occurs at the base of both sections. Therefore, we conclude that the dominance of the ultrastable suite Ap-Tur-Zrn-Rt in the Jaca wedge-top basin reflects the abundance of these minerals in their source rocks rather than a strong diagenetic feature experienced by the sedimentary infill of the Jaca basin. Furthermore, the Jaca foreland basin is an example that sediment recycling increases the ZTR relative abundance in the sedimentary record, although additional crystalline sources were being eroded at the same time.

The occurrence of unstable minerals in all of the upper Eocene to Miocene alluvial fans implies the uplift and contribution of source areas consisting of the Paleozoic and Mesozoic metamorphic and igneous terrains as the source of the more unstable minerals, at the same time that the former turbidite basin was being eroded. The integration of heavy-mineral analysis with sandstone petrography allowed a better characterization of the source rocks and helped to point to probable specific source areas located in the North Pyrenean Zone or the northern Axial Zone of the Pyrenees as the Lesponne or Barousse crystalline massifs.

Our findings reinforce the idea that during the late Eocene the drainage divide of the transverse drainage system north of the Jaca basin extended to the North Pyrenean Zone, and to some local areas of the Axial Zone basement exposed in the west-central Pyrenees.

Our results also show that the heavy-mineral suites of the Belsué-Atarés and the fluvial Campodarbe formations, giving evidence for that stratigraphic correlations with the fluvial and alluvial systems of the Aínsa basin should be revisited, new sediment pathways should be considered, or further research is needed regarding the heavy-mineral provenance signature of both basins.

From our data, we infer that epidote is sourced mainly from Triassic dolerites (ophites) that have gone through spilitization. The epidote occurrence in the Jaca basin takes place first in the eastern segment, in the older alluvial deposits (Canciás fan, Oligocene), and later in the youngest San Juan de la

Peña fan (Oligocene-Miocene) located in the westernmost part of the basin. Since this trend is also observed in the nearby Tremp-Graus basin, the epidote occurrence in the South-Pyrenean basin is diachronic from east to west and therefore highlights the east-west propagation of Pyrenean deformation.

AKNOWLEGMENTS

This paper is a contribution to the projects CGL2014-54180-P and PGC2018-093903-B-C21, financed by the Ministerio de Economia y Competitividad (MINECO) and Ministerio de Ciencia, Inovación y Universidades (MCIU) of Spain. X. Coll acknowledges support from the Ministerio de Cultura, Deporte y Educacción (MCDE) of Spain (FPU grant). We are very grateful to the reviewers Eric Lasseur and Sergio Andò, and to the editor John Southard, for providing constructive reviews that helped to improve the original paper.

REFERENCES

Andò, S., 2020, Gravimetric separation of heavy minerals in sediments and rocks: Minerals, v. 10, p. 273.

Andò, S., and Garzanti, E., 2014, Raman spectroscopy in heavy-mineral studies, *in* Scott, R., Smyth, H., Morton, A., and Richardson, N., eds., Sediment Provenance Studies, in Hydrocarbon Exploration and Production: Geological Society of London, Special Publication 386, p. 395–412.

Andò, S., Garzanti, E., Padoan, M., and Limonta, M., 2012, Corrosion of heavy minerals during weathering and diagenesis: A catalog for optical analysis: Sedimentary Geology, v. 280, p. 165–178.

Andò, S., Morton, A., and Garzanti, E., 2014, Metamorphic grade of source rocks revealed by chemical fingerprints of detrital amphibole and garnet, *in* Scott, R., Smyth, H., Morton, A., and Richardson, N., eds., Sediment Provenance Studies, in Hydrocarbon Exploration and Production: Geological Society of London, Special Publication 386, p. 351–371.

Andò, S., Aharonovich, S., Hahn, A., George, S.C., Clift, P.D., and Garzanti, E., 2019, Integrating heavy-mineral, geochemical and biomarker analyses of Plio-Pleistocene sandy and silty turbidites: a novel approach for provenance studies (Indus Fan, IODP Expedition 355): Geological Magazine, v. 157, p. 1–10.

Azambre, B., 1967, Sur les roches intrusives sous-saturées du Crétacé des Pyrénées: Séances de l'Académie des Sciences, Comptes Rendus Hebdomadaires, v. 271, p. 641–643.

Azambre, B., Rossy, M., and Lago, M., 1987. Caracteristiques petrologiques des dolerites tholeiitiques d'age triasique (ophites) du domaine pyreneen: Bulletin de Minéralogie, v. 110, p. 379–396.

Azambre, B., Crouzel, F., Debroas, E.J., Soulé, J.C., and Ternet, Y., 1989, Notice explicative de la Carte géologique de la France (1/50000) feuille Bagnères-de-Bigorre (1053): Bureau des Recherches Géologiques et Minières Orléans.

Babault, J., van den Driessche, J., and Teixell, A., 2011, Retro- to pro-side migration of the main drainage divide in the Pyrenees: geologic and geomorphological evidence: European Geosciences Union General Assembly EGU, v. 13, p. 2011–12567.

Barnolas, A., and Gil-Peña, I., 2001, Ejemplos de relleno sedimentario multiepisódico en una cuenca de antepaís fragmentada: La Cuenca Surpirenaica: Boletín Geológico y Minero, v. 112, p. 17–38.

Barsó, D., 2007, Análisis de la procedencia de los conglomerados sinorogénicos de La Pobla de Segur (Lérida) y su relación con la evolución tectónica de los Pirineos centro meridionales durante el Eoceno medio-Oligoceno [PhD Thesis]: Universitat de Barcelona, Barcelona, Spain, 209 p.

Beamud, E., Garcés, M., Cabrera, L., Muñoz, J.A., and Almar, Y., 2003, A new middle to late Eocene continental chronostratigraphy from NE Spain: Earth and Planetary Science Letters, v. 216, p. 501–514.

Bentham, P.A., Burbank, D.W., and Puigdefàbregas, C., 1992, Temporal and spatial controls on the alluvial architecture of an axial drainage system: late Eocene Escanilla Formation, southern Pyrenean foreland basin, Spain: Basin Research, v. 4, p. 335–352.

Bixel, F., 1987, Le volcanisme stéphano-permien des Pyrénées. Pétrographie, minéralogie, géochimie: Cuadernos de Geología Ibérica, v. 11, p. 41–55.

Bosch, G.V., Teixell, A., Jolivet, M., Labaume, P., Stockli, D., Domènech, M., and Monié, P., 2016, Timing of Eocene–Miocene thrust activity in the Western Axial Zone and Chaînons Béarnais (west-central Pyrenees) revealed by multi-method thermochronology: Comptes Rendus Geoscience, v. 348, p. 246–256.

Boya, S., 2018, El sistema deltaico de la Arenisca de Sabiñánigo y la continentalización de la cuenca de Jaca [PhD Thesis]: Universitat Autònoma de Barcelona, Barcelona, Spain, 231 p.

Caja, M.A., Marfil, R., Garcia, D., Remacha, E., Morad, S., Mansurbeg, H., Amorosi, A., Martínez-Calvo, C., and Lahoz-Beltrá, R., 2010, Provenance of siliciclastic and hybrid turbiditic arenites of the Eocene Hecho Group, Spanish Pyrenees: implications for the tectonic evolution of a foreland basin: Basin Research, v. 22, p. 157–180.

Caracciolo, L., Garzanti, E., von Eynatten, H., and Weltje, G.J., 2016, Sediment generation and provenance: processes and pathways: Sedimentary Geology, v. 336, p. 1–2.

Caracciolo, L., Andò, S., Vermeesch, P., Garzanti, E., McCabe, R., Barbarano, M., Paleari, C., Rittner, M., and Pearce, T., 2019, A multidisciplinary approach for the quantitative provenance analysis of siltstone: Mesozoic Mandawa Basin, southeastern Tanzania, *in* Bond, C.E., and Lebit, H.D., eds., Folding and Fracturing of Rocks: 50 Years of Research since the Seminal Text Book of J. G. Ramsay: Geological Society of London, Special Publication, v. 484. p. 275–293.

Cerveny, P.F., Johnson, N.M., Tahirkheli, R.A.K., and Bonis, N.R. 1989, Tectonic and geomorphic implications of Siwalik Group heavy minerals, Potwar Plateau, Pakistan, *in* Malinconico, L.L., and Lillie, R.J., eds., Tectonics of the western Himalayas: Geological Society of America, Special Papers, v. 232, p. 129–136.

Clerc, C., Lahfid, A., Monié, P., Lagabrielle, Y., Chopin, C., Poujol, M., Boulvais, P., Ringenbach, J.C., Masini, E. and de St Blanquat, M., 2015, High-temperature metamorphism during extreme thinning of the continental crust: a reappraisal of the North Pyrenean passive paleomargin: Solid Earth, v. 6, p. 643–668.

Coll, X., Gómez-Gras, D., Roigé, M., and Mestres, N., 2017, Heavy-mineral assemblages as a provenance indicator in the Jaca basin (Middle-Late Eocene, southern Pyrenees): Geogaceta, v. 61 p. 159–162.

Coll, X., Gómez-Gras, D., Roigé, M., Boya, S., Teixell, A., and Poyatos-Moré, M., 2019, Interplay of Multiple Sediment Sources in an Overfilled Foreland Basin (Southern Pyrenees) [Abstract]: International Association of Sedimentologists, 34th International Meeting of Sedimentology, Abstracts, p. 872.

Costa, E., Garces, M., López-Blanco, M., Beamud, E., Gómez-Paccard, M., and Larrasoaña, J.C., 2010, Closing and continentalization of the South Pyrenean foreland basin (NE Spain): magnetochronological constraints: Basin Research, v. 22, p. 904–917.

Crognier, N., 2016, Évolution thermique, circulation de fluides et fracturation associées à la structuration du bassin d'avant-pays sud-pyrénéen [PhD Thesis]: l'Université de Pau et des Pays de l'Adour, Pau, France, 344 p.

Debon, F., Enrique, P., and Autran, A., 1996, Le plutonisme hercynien des Pyrénées, *in* Barnolas, A., and Chiron, J., eds., Synthèse géologique et géophysique des Pyrénées: Bureau de Recherches Géologiques et Minières-Instituto Tecnologico Geominero de España, p. 361–499.

Dickinson, W.R., and Suczek, C.A., 1979, Plate tectonics and sandstone compositions: American Association of Petroleum Geologists, Bulletin v. 63, p. 2164–2182.

Dickinson, W.R., 1988, Provenance and sediment dispersal in relation to paleotectonics and paleogeography of sedimentary basins, *in* Kleinspehn, K.L., and Paola, C., eds., New Perspectives in Basin Analysis: Berlin, Springer, p. 3–25.

Dreyer, T., Corregidor, J., Arbues, P., and Puigdefabregas, C., 1999, Architecture of the tectonically influenced Sobrarbe deltaic complex in the Ainsa Basin, northern Spain: Sedimentary Geology, v. 127, p. 127–169.

Fontana, D., Zuffa, G.G., and Garzanti, E., 1989, The interaction of eustacy and tectonism from provenance studies of the Eocene Hecho Group Turbidite Complex (South-Central Pyrenees, Spain): Basin Research, v. 2, p. 223–237.

Fossum, K., Morton, A.C., Dypvik, H., and Hudson, W.E., 2019, Integrated heavy mineral study of Jurassic to Paleogene sandstones in the Mandawa Basin, Tanzania: Sediment provenance and source-to-sink relations: Journal of African Earth Sciences, v. 150, p. 546–565.

Galehouse, J., 1971, Point counting, *in* Carver, R., ed., Procedures in Sedimentary Petrology: New York, Wiley, p. 385–407.

Garcés, M., López-Blanco, M., Valero, L., Beamud, E., Muñoz, J.A., Oliva-Urcia, B., Vinyoles, A., Arbués, P., Cabello, P., and Cabrera, L., 2020, Paleogeographic and sedimentary evolution of the south-pyrenean foreland basin: Marine and Petroleum Geology, v. 113, p. 104105.

Garzanti, E., 2016, From static to dynamic provenance analysis—Sedimentary petrology upgraded: Sedimentary Geology, v. 336, p. 3–13.

Garzanti, E., and Andò, S., 2007a, Heavy mineral concentration in modern sands: implications for provenance interpretation, *in* Mange, M.A., and Wright, D.T., eds., Heavy Minerals in Use: Amsterdam, Elsevier, Developments in Sedimentology Series 58, p. 517–545.

Garzanti, E., and Andò, S., 2007b, Plate tectonics and heavy mineral suites of modern sands, *in* Mange, M.A., and Wright, D.T., eds., Heavy Minerals in Use: Amsterdam, Elsevier, Developments in Sedimentology Series 58, p. 741–763.

Garzanti, E., and Andò, S., 2019, Heavy Minerals for Junior Woodchucks: Minerals, v. 8, p. 148–172.

Garzanti, E., Ando, S., Vezzoli, G., and Dell'era, D., 2003, From Rifted Margins to Foreland Basins: Investigating Provenance and Sediment Dispersal Across Desert Arabia (Oman, U.A.E.): Journal of Sedimentary Research, v. 73, p. 572–588.

Garzanti, E., Vezzoli, G., Lombardo, B., Andò, S., Mauri, E., Monguzzi, S., and Russo, M., 2004, Collision-Orogen Provenance (Western Alps): Detrital Signatures and Unroofing Trends: The Journal of Geology, v. 112, p. 145–164.

Garzanti, E., Andò, S., and Vezzoli, G., 2006, The Continental Crust as a Source of Sand (Southern Alps Cross Section, Northern Italy): The Journal of Geology, v. 114, p. 533–554.

Garzanti, E., Doglioni, C., Vezzoli, G., and Andò, S., 2007, Orogenic Belts and Orogenic Sediment Provenance: The Journal of Geology, v. 115, p. 315–334.

Garzanti, E., Andò, S., and Vezzoli, G., 2008, Settling equivalence of detrital minerals and grain-size dependence of sediment composition: Earth and Planetary Science Letters, v. 273, p. 138–151.

Garzanti, E., Andò, S., and Vezzoli, G., 2009, Grain-size dependence of sediment composition and environmental bias in provenance studies: Earth and Planetary Science Letters, v. 277, p. 422–432.

Garzanti, E., Resentini, A., Vezzoli, G., Andò, S., Malusà, M., and Padoan, M., 2012, Forward compositional modelling of Alpine orogenic sediments: Sedimentary Geology, v. 280, p. 149–164.

Garzanti, E., Limonta, M., Resentini, A., Bandopadhyay, P.C., Najman, Y., Andò, S., and Vezzoli, G., 2013a, Sediment recycling at convergent plate margins (Indo-Burman Ranges and Andaman–Nicobar Ridge): Earth-Science Reviews, v. 123, p. 113–132.

Garzanti, E., Padoan, M., Andò, S., Resentini, A., Vezzoli, G., and Lustrino, M., 2013b, Weathering and Relative Durability of Detrital Minerals in Equatorial Climate: Sand Petrology and Geochemistry in the East African Rift: The Journal of Geology, v. 121, p. 547–580.

Garzanti, E., Vermeesch, P., Padoan, M., Resentini, A., Vezzoli, G., and Andò, S., 2014, Provenance of Passive-Margin Sand (Southern Africa): The Journal of Geology, v. 122, p. 17–42.

Garzanti, E., Andò, S., Limonta, M., Fielding, L., and Najman, Y., 2018, Diagenetic control on mineralogical suites in sand, silt, and mud (Cenozoic Nile Delta): Implications for provenance reconstructions: Earth-Science Reviews, v. 185, p. 122–139.

Gilbert, J.S., and Rogers, N.W., 1989, The significance of garnet in the Permo-Carboniferous volcanic rocks of the Pyrenees: Geological Society of London, Journal, v.146, p. 477–490.

Golberg, J.M., and Leyreloup, A.F., 1990, High temperature-low pressure Cretaceous metamorphism related to crustal thinning (Eastern North Pyrenean Zone, France): Contributions to Mineralogy and Petrology, v. 104, p. 19–207.

Gómez-Gras, D., Roigé, M., Fondevilla, V., Oms, O., Boya, S., and Remacha, E., 2016, Provenance constraints on the Tremp Formation paleogeography (southern Pyrenees): Ebro Massif VS Pyrenees sources: Cretaceous Research, v. 57, p. 414–427.

Gómez-Gras, D., Collado, R., Coll, X., and Roigé, M., 2017, Compositional characterization of the Upper Cretaceous sandstones in the Sierras Marginales y Exteriores (south-Pyrenean basin): Heavy-mineral and sandstone petrography analysis: Geogaceta, v. 61, p. 163–166.

Götze, J., 1998, Geochemistry and provenance of the Altendorf feldspathic sandstone in the Middle Bunter of the Thuringian basin (Germany): Chemical Geology, v. 150, p. 43–61.

Graham, S.A., Tolson, R.B., DeCelles, P.G., Ingersoll, R.V., Bargar, E., Caldwell, M., Cavazza, W., Edwards, D.P., Follo, M.F., Handschy, J.F., Lemke, L., Moxon, I., Rice, R., Smith, G. A., and White, J., 1986, Provenance modelling as a technique for analysing source terrane evolution and controls on foreland sedimentation, *in* Allen, P.A., and Homewood, P.N., eds., Foreland Basins: International Association of Sedimentologists, Special Publication 8, p. 425–436.

Greenacre, M., 1984, Theory and applications of correspondence analysis: London, Academic press, 364 p.

Guitard, G., Vielzeuf, D., and Martinez, F., 1996, Métamorphisme hercynien, *in* Barnolas, A., and Chiron, J., eds., synthèse géologique et géophysique des Pyrénées: Bureau de Recherches Géologiques et Minières-Instituto Tecnologico Geominero de España. p. 501–584.

Gupta, K.D., and Pickering, K.T., 2008, Petrography and temporal changes in petrofacies of deep-marine Ainsa-Jaca basin sandstone systems, Early and Middle Eocene, Spanish Pyrenees: Sedimentology, v. 55, p. 1083–1114.

Harris, N.B.W., 1974, The petrology and petrogenesis of some muscovite granite sills from the Barousse Massif, Central Pyrenees: Contributions to Mineralogy and Petrology, v. 45, p. 215–230.

Haughton, P.D.W., Todd, S.P., and Morton, A.C., 1991, Sedimentary provenance studies, *in* Haughton, P.D.W., Todd, S.P., and Morton, A.C., eds., Developments in Sedimentary Provenance Studies: Geological Society of London, Special Publication 57, p. 1–11.

Hirst, J.P.P., and Nichols, G.J., 1986, Thrust tectonic controls on Miocene alluvial distribution patterns, southern Pyrenees, *in* Allen, P.A., and Homewood, P., eds., Foreland Basins: International Association of Sedimentologists, Special Publication 8, p. 247–258.

Hogan, P., 1993, Geochronologic, Tectonic and Stratigraphic Evolution of the Southwest Pyrenean Foreland Basin, Northern Spain [PhD Thesis]: University of Southern California, Los Angeles, U.S.A., 208 p.

Hogan, P.J., and Burbank, D.W., 1996, Evolution of the Jaca Piggyback Basin and emergence of the external sierra, Southern Pyrenees, *in* Friend, P., and Dabrio, C., eds., Tertiary Basins of Spain: Cambridge, Cambridge University Press, p. 153–160.

Jolivet, M., Labaume, P., Monié, P., Brunel, M., Arnaud, N., and Campani, M., 2007, Thermochronology constraints for the propagation sequence of the south Pyrenean basement thrust system (France-Spain): Tectonics, v. 26, p. TC5007.

Kilhams, B., Morton, A., Borella, R., Wilkins, A., and Hurst, A., 2014, Understanding the provenance and reservoir quality of the Sele Formation sandstones of the UK Central Graben utilizing detrital garnet suites, in Scott, R.A., Smyth, H.R., Morton, A.C., and Richardson, N., eds., Sediment Provenance Studies in Hydrocarbon Exploration and Production: Geological Society of London, Special Publications 386, p. 129–142.

Kuebler, K.E., Jolliff, B.L., Wang, A., and Haskin, L.A. 2006, Extracting olivine (Fo–Fa) compositions from Raman spectral peak positions: Geochimica et Cosmochimica Acta, v. 70, p. 6201–6222.

Labaume, P., and Teixell, A., 2018, 3D structure of subsurface thrusts in the eastern Jaca Basin, southern Pyrenees: Geologica Acta, v. 16, p. 477-498.

Labaume, P., Séguret, M., and Seyve, C., 1985, Evolution of a turbiditic foreland basin and analogy with an accretionary prism: Example of the Eocene South-Pyrenean Basin: Tectonics, v. 4, p. 661–685.

Labaume, P., Meresse, F., Jolivet, M., Teixell, A., and Lahfid, A., 2016a, Tectonothermal history of an exhumed thrust-sheet-top basin: An example from the south Pyrenean thrust belt: Tectonics, v. 35, p. 1280–1313.

Labaume, P., Meresse, F., Jolivet, M., and Teixell, A., 2016b, Exhumation sequence of the basement thrust units in the west-central Pyrenees. Constraints from apatite fission track analysis: Geogaceta, v. 60, p. 11–14.

Lagabrielle, Y., Labaume, P., and de Saint Blanquat, M., 2010, Mantle exhumation, crustal denudation, and gravity tectonics during Cretaceous rifting in the Pyrenean realm (SW Europe): Insights from the geological setting of the lherzolite bodies: Tectonics, v. 29, p. TC4012.

Lago, M., Galé, C., Arranz, E., Vaquer, R., Gil, A., and Pocovi, A., 2000, Triassic tholeiitic dolerites («ophites») of the El Grado diapir: Estudios geológicos, v. 56, p. 3–8.

Lihou, J.C., and Mange-Rajetzky, M.A., 1996, Provenance of the Sardona Flysch, eastern Swiss Alps: example of high-resolution heavy mineral analysis applied to an ultrastable assemblage: Sedimentary Geology, v. 105, p. 141–157.

Majesté-Menjoulás, C., Debon, F., and Barrère, P., 1999, Notice explicative de la Carte géologique de la France (1/50000), feuille Gavarnie (1082): Bureau des Recherches Géologiques et Minières Orléans.

Mange, M.A., and Maurer, H.F.W., 1992, Heavy Minerals in Colour: London, Chapman and Hall, 147 p.

Mange, M.A., Dewey, J.F., and Wright, D.T., 2003, Heavy minerals solve structural and stratigraphic problems in Ordovician strata of the western Irish Caledonides: Geological Magazine, v. 140, p. 25–30.

Mange-Rajetzky, M.A., 1995, Subdivision and correlation of monotonous sandstone sequences using high-resolution heavy mineral analysis, a case study: the Triassic of the Central Graben, *in* Dunay, R.E., and Hailwood, E.A., eds., Non-biostratigraphical Methods of Dating and Correlation: Geological Society of London, Special Publication 89, p. 23–30.

Mangin, J., 1960, Le Nummulitique Sud-Pyrénéen à l'ouest de l'Aragón: Pirineos v. 51–58, p. 77–111.

McKellar, Z., Hartley, A.J., Morton, A.C., and Frei, D., 2020, A multidisciplinary approach to sediment provenance analysis of the late Silurian–Devonian Lower Old Red Sandstone succession, northern Midland Valley Basin, Scotland: Geological Society of London, Journal, v. 177, p. 297–314.

Meresse, F., 2010, Dynamique d'un prisme orogénique intracontinental: évolution thermochronologique (traces de fission sur apatite) et tectonique de la Zone Axiale et des piémonts des Pyrénées centrooccidentales [PhD Thesis]: Université de Montpellier 2, Montpellier, France, 280 p.

Michael, N., 2013, Functioning of an Ancient Routing System, the Escanilla Formation, South Central Pyrenees [PhD Thesis]: Imperial College London, London, U.K., 284 p.

Milliken, K.L., 2007, Provenance and diagenesis of heavy minerals, Cenozoic units of the northwestern Gulf of Mexico sedimentary basin, *in* Mange, M.A., and Wright, D.T., eds., Heavy Minerals in Use: Amsterdam, Elsevier, Developments in Sedimentology Series 58, p. 247–261.

Milliken, K.L., and Mack, L.E., 1990, Subsurface dissolution of heavy minerals, Frio Formation sandstones of the ancestral Rio Grande Province, South Texas: Sedimentary Geology, v. 68, p. 187–199.

Montes, M., and Colombo, F., 1996, Análisis secuencial y correlación de los abanicos aluviales de Peña Oroel y la Sierra de Cancias (Eoceno superior. Cuenca Surpirenaica Central): Geogaceta, v. 20, p. 76–79.

Morris, R.G., Sinclair, H.D., and Yelland, A.J., 1998, Exhumation of the Pyrenean orogen: implications for sediment discharge: Basin Research, v. 10, p. 69-85.

Morton, A.C., 1984, Stability of detrital heavy minerals in Tertiary sandstones from the North Sea Basin: Clay Minerals, v. 19, p. 287–308.

Morton, A.C., and Hallsworth, C., 1999, Processes controlling the composition of heavy mineral assemblages in sandstones: Sedimentary Geology, v. 124, p. 3–29.

Morton, A.C., and Hallsworth, C., 2007, Stability of detrital heavy minerals during burial diagenesis, *in* Mange, M.A., and Wright, D.T., eds., Heavy Minerals in Use: Amsterdam, Elsevier, Developments in Sedimentology Series 58, p. 215–245.

Morton, A.C., Hallsworth, C., and Chalton, B., 2004, Garnet compositions in Scottish and Norwegian basement terrains: a framework for interpretation of North Sea sandstone provenance: Marine and Petroleum Geology, v. 21, p. 393–410.

Morton, A.C., Humphreys, B., and Dharmayanti, D.A., 1994, Palaeogeographic implications of the heavy mineral distribution in Miocene sandstones of the North Sumatra Basin: Journal of Southeast Asian Earth Sciences, v. 10, p. 177–190.

Mouthereau, F., Filleaudeau, P.Y., Vacherat, A., Pik, R., Lacombe, O., Fellin, M.G., Castelltort, S., Christophoul, F., and Masini, E., 2014, Placing limits to shortening evolution in the Pyrenees: Role of margin architecture and implications for the Iberia/Europe convergence: Tectonics, v. 33, p. 2283–2314.

Muñoz, J.A., 1992, Evolution of a continental collision belt: ECORS-Pyrenees crustal balanced cross-section, *in* McClay K.R., ed., Thrust Tectonics: London, Chapman & Hall, p. 235–246.

Mutti, E., 1985, Turbidite systems and their relations to depositional sequences, *in* Zuffa, G.G., ed., Provenance of Arenites: Dordrecht, Springer, p. 65–93.

Mutti, E., Remacha, E., Rosell, J., Valloni, R., and Zamorano, M., 1985, Stratigraphy and facies characteristics of the Eocene Hecho group turbidite systems, South-Central Pyrenees, *in*: International Association of Sedimentologists 6th European regional meeting, Lleida, Field Trip 12 Guidebook, p. 519–576.

Nie, J., Horton, B.K., Saylor, J.E., Mora, A., Mange, M., Garzione, C.N., Basu, A., Moreno, C.J., Caballero, V., and Parra, M., 2012, Integrated provenance analysis of a convergent retroarc foreland system: U–Pb ages, heavy minerals, Nd isotopes, and sandstone compositions of the Middle Magdalena Valley basin, northern Andes, Colombia: Earth-Science Reviews, v. 110, p. 111–126.

Nijman, W., and Nio, S., 1975, The Eocene Montañana Delta (Tremp-Graus Basin, provinces of Lérida and Huesca, Southern Pyrenees, N Spain), Field Trip B Guidebook (The Sedimentary Evolution of the Paleogene South Pyrenean Basin): International Association of Sedimentologists, XI International Sedimentological Congress, Excursion Guidebook. p. 1–20.

Oliva-Urcia, B., Beamud, E., Garcés, M., Arenas, C., Soto, R., Pueyo, E.L., and Pardo, G., 2016, New magnetostratigraphic dating of the Palaeogene syntectonic sediments of the west-central Pyrenees: tectonostratigraphic implications, *in* Pueyo, E.L., Cifelli, F., Sussman, A.J., and Oliva-Urcia, B., eds., Palaeomagnetism in Fold and Thrust Belts: New Perspectives: Geological Society of London, Special Publication 425, p. 107–128.

Oms, O., Dinarès-Turell, J., and Remacha, E., 2003, Magnetic stratigraphy from deep clastic turbidites: an example from the Eocene Hecho group (southern Pyrenees): Studia Geophysica et Geodaetica, v. 47, p. 275–288.

Ortí, F., Salvany, J.M., Rosell, L., Pueyo, J.J., and Inglés, M., 1986, Evaporitas antiguas (Navarra) y actuales (Los Manegros) de la Cuenca del Ebro, *in* Anadón, P., and Cabrera, L., eds., Guía de Las Excursiones Del XI Congreso Español de Sedimentologia: Generalitat de Catalunya, Comissió Interdepartamental de Recerca i Innovació Tecnològica (CIRIT), Barcelona. p. 21–21.

Ortuño, M., and Viaplana-Muzas, M., 2018, Active fault control in the distribution of Elevated Low Relief Topography in the Central-Western Pyrenees: Geologica Acta, v. 16, p. 499–518.

Payros, A., Pujalte, V., and Orue-Etxebarria, X., 1999, The South Pyrenean Eocene carbonate megabreccias revisited: new interpretation based on evidence from the Pamplona Basin: Sedimentary Geology, v. 125, p. 165–194.

Pouget, P., 1989, Évolution géodynamique hercynienne des Pyrénées centrales. Contraintes structurales métamorphiques, magmatiques et sédimentologiques [PhD Thesis]: Université Toulouse III Paul Sabatier, Toulouse, France.

Puigdefàbregas, C., 1975, La sedimentación molásica en la cuenca de Jaca: Pirineos, v. 104, p. 1–188.

Puigdefàbregas, C., Muñoz, J.A., and Vergés, J., 1992, Thrusting and foreland basin evolution in the southern Pyrenees, *in* McClay K.R., ed., Thrust Tectonics: London, Chapman & Hall, p. 247–254.

Recio, J.M., Torres-Girón, M.L., and García-Ruiz, J M., 1987, Genetical and physicochemical aspects of the silty deposits of Monte Perdido Massif: Pirineos, v. 160, p. 95–103.

Remacha, E., and Fernández, L.P., 2003, High-resolution correlation patterns in the turbidite systems of the Hecho Group (South-Central Pyrenees, Spain), *in* Mutti, E., Steffens, G.S., Pirmez, C., Orlando, M., and Roberts, D., eds., Turbidites: Models and Problems: Marine and Petroleum Geology, v. 20, p. 711–726.

Remacha, E., Oms, O., and Coello, J., 1995, The Rapitán turbidite channel and its related eastern levee-overbank deposits, Eocene Hecho group, south-central Pyrenees, Spain, *in* Pickering, K., Hiscott, R., Kenyon, N., Ricci Lucchi, F., and Smith, R., eds., Atlas of Deep Water Environments: Architectural Style in Turbidite Systems: London, Chapman and Hall, p. 145–149.

Remacha, E., Fernandez, L.P., and Maestro, E., 2005, The Transition Between Sheet-Like Lobe and Basin-Plain Turbidites in the Hecho Basin (South-Central Pyrenees, Spain): Journal of Sedimentary Research, v. 75, p. 798–819.

Reynolds, A.D., 1987, Tectonically controlled alluvial sedimentation in the South Pyrenean foreland basin [PhD Thesis]: University of Liverpool, Liverpool, U.K., 309 p.

Ribeiro, M.L., Reche, J., López-Carmona, A., and Quesada, C., 2019, Variscan Metamorphism, *in* Quesada, C., and Oliveira, J.T., eds., The Geology of Iberia: A Geodynamic Approach: Regional Geology Reviews, Springer, p. 473–498.

Ríos Aragüés, L.M., Lanaja del Busto, J.M., Ríos Mitchell, J.M. and Marín Blanco, F.J., 1982, Mapa geológico de España 1:50.000, hoja nº179 (Bielsa) y memoria. Instituto Geológico y Minero de España Madrid.

Roigé, M., 2018, Procedència i evolució dels sistemes sedimentaris de la conca de Jaca (conca d'avantpaís Sudpirinenca): Interacció entre diverses àrees font en un context tectònic actiu. [PhD Thesis]: Universitat Autònoma de Barcelona, Barcelona, Spain, 312 p.

Roigé, M., Gómez-Gras, D., Remacha, E., Daza, R., and Boya, S., 2016, Tectonic control on sediment sources in the Jaca basin (Middle and Upper Eocene of the South-Central Pyrenees): Comptes Rendus Geoscience, v. 348, p. 236–245.

Roigé, M., Gómez-Gras, D., Remacha, E., Boya, S., Viaplana-Muzas, M., and Teixell, A., 2017, Recycling an uplifted early foreland basin fill: An example from the Jaca basin (Southern Pyrenees, Spain): Sedimentary geology, v. 360, p. 1–21.

Roigé, M., Gómez-Gras, D., Stockli, D.F., Teixell, A., Boya, S., and Remacha, E., 2019, Detrital zircon U–Pb insights into the timing and provenance of the South Pyrenean Jaca basin: Geological Society of London, Journal, v. 176, p. 1182–1190.

Roure, F., Choukroune, P., Berastegui, X., Muñoz, J.A., Villien, A., Matheron, P., Bareyt, M., Seguret, M., Camara, P., and Deramond, J., 1989, Ecors deep seismic data and balanced cross sections: Geometric constraints on the evolution of the Pyrenees: Tectonics, v. 8, p. 41–50.

Rubio, V., Vigil, R., García, R., and González, J.A., 1996, Caracterización mineralógica de sedimentos arenosos en la cuenca del río Ara (Huesca): Cuaternario y Geomorfología, v. 10, p. 33–44.

Souquet, P., 1967, Le Crétacé Supérieur Sud-Pyrénées en Catalogne, Aragon et Navarra [PhD Thesis]: Université de Toulouse, Toulouse, France, 529 p.

Steidtmann, J.R., and Schmitt, J.G., 1988, Provenance and Dispersal of Tectogenic Sediments in Thin-Skinned, Thrusted Terrains, *in* Kleinspehn, K.L., and Paola, C., eds., New Perspectives in Basin Analysis: New York, Springer-Verlag, p. 353–366.

Teixell, A., 1996, The Ansó transect of the southern Pyrenees: basement and cover thrust geometries: Geological Society of London, Journal, v. 153, p. 301–310.

Teixell, A., 1998, Crustal structure and orogenic material budget in the west central Pyrenees: Tectonics, v. 17, p. 395–406.

Ternet, Y., Barrere, P., and Debroas, E.J., 1995, Notice explicative de la Carte géologique de la France (1/50000), feuille Campan (1071): Bureau des Recherches Géologiques et Minières Orléans.

Uddin, A., Kumar, P., Sarma, J.N., and Akhter, S.H., 2007, Heavy mineral constraints on the provenance of Cenozoic sediments from the foreland basins of Assam and Bangladesh: erosional history of the eastern Himalayas and the Indo-Burman Ranges, *in* Mange, M.A., and Wright, D.T., eds., Heavy Minerals in Use: Amsterdam, Elsevier, Developments in Sedimentology Series 58, p. 823–847.

Ullastre, J., and Masriera, A., 1982, Hipótesis y problemas acerca del origen de las Asociaciones de minerales pesados del Senoniense del Pirineo Catalán: Cuadernos de Geología Ibérica, v. 8, p. 949–964.

Vacherat, A., Mouthereau, F., Pik, R., Bernet, M., Gautheron, C., Masini, E., Pourhiet, L.L., Tibari, B., and Lahfid, A., 2014, Thermal imprint of rift-related processes in orogens as recorded in the Pyrenees: Earth and Planetary Science Letters, v. 408, p. 296–306.

Valloni, R., Marchi, M., and Mutti, E., 1984, Studio conoscitivo della moda detritica delle torbiditi eoceniche del Gruppo di Echo (Spagna): Giornale di Geologia, v. 46, p. 45–56.

Velbel, M. A., 2007, Surface textures and dissolution processes of heavy minerals in the sedimentary cycle: examples from pyroxenes and amphiboles, *in* Mange, M.A., and Wright, D.T., eds., Heavy Minerals in Use: Amsterdam, Elsevier, Developments in Sedimentology Series 58, p. 113–150.

Vergés, J., Fernàndez, M., and Martìnez, A., 2002, The Pyrenean orogen: pre-, syn-, and post-collisional evolution: Journal of the Virtual Explorer, v. 08, p. 55–74.

Vermeesch, P., 2018, Statistical models for point-counting data: Earth and Planetary Science Letters, v. 501, p. 112–118.

Vermeesch, P., Resentini, A., and Garzanti, E., 2016, An R package for statistical provenance analysis: Sedimentary Geology, v. 336, p. 14–25.

Vincent, S.J., 2001, The Sis paleovalley a record of proximal fluvial sedimentation and drainage basin development in response to Pyrenean mountain building: Sedimentology, v. 48, p. 1235–1276.

von Eynatten, H., and Dunkl, I., 2012, Assessing the sediment factory: the role of single grain analysis: Earth Science Reviews, v. 115, p. 97–120.

von Eynatten, H., and Gaupp, R., 1999, Provenance of Cretaceous synorogenic sandstones in the Eastern Alps: constraints from framework petrography, heavy mineral analysis and mineral chemistry: Sedimentary Geology, v. 124, p. 81–111.

Walderhaug, O., and Porten, K.W., 2007, Stability of Detrital Heavy Minerals on the Norwegian Continental Shelf as a Function of Depth and Temperature: Journal of Sedimentary Research, v. 77, p. 992–1002.

Wang, A., Kuebler, K.E., Jolliff, B.L., & Haskin, L.A., 2004, Raman spectroscopy of Fe-Ti-Cr-oxides, case study: Martian meteorite EETA79001: American Mineralogist, v. 89, p.665–680.

Yuste, A., Bauluz, B., and Luzón, A., 2006, Asociaciones características de minerales pesados en las areniscas del borde septentrional de la cuenca del Ebro (zona central): Macla: Sociedad Española de Mineralogía, Revista, v. 6, p. 501–504.

Zwart, H.J., 1986, The Variscan geology of the Pyrenees: Tectonophysics, v, 129, p. 9–27.

Zwart, H.J., and Sitter, L.D., 1979, The geology of the Central Pyrenees: Leidse Geologische Mededelingen, v. 50, p. 1–74.

FIGURE CAPTIONS

Fig. 1. A) Simplified geological map of the Pyrenees (redrawn from Teixell, 1996), showing the location of the study area (white frame). White line indicates cross-section in Part B. Lk: Lakora thrust; Ga: Gavarnie thrust. B) Crustal cross section of the west-central Pyrenees (simplified from Teixell et al., 2016), showing both the South Pyrenean Zone and the North Pyrenean Zone. NPFT: North-Pyrenean Frontal Thrust; BU: Bedous Triassic Unit.

Fig. 2. A) Geological map of the northern sector of the Jaca basin (modified from Roigé et al., 2017). Purple lines show the location of the stratigraphic sections represented in Fig. 6. B) General stratigraphic

cross-section sketch summarizing the relationships of the analyzed deposits (modified from Roigé et al., 2017). Stratigraphic ages are extracted from Labaume et al. (1985), Hogan and Burbank (1996), Oms et al. (2003), and Roigé et al (2019). Blue-purple bars indicate the position of the measured stratigraphic logs in this work (for interpretation of the references to color in this figure legend, the reader is referred to the web version of this article).

Fig. 3. Geological map of the Pyrenees showing the potential sources of heavy minerals (modified from Roigé et al., 2017).

Fig. 4. Representative Raman spectra of heavy minerals from the late Eocene-Miocene Jaca basin.

Fig. 5. Representative Raman spectra of heavy minerals from the late Eocene-Miocene Jaca basin.

Fig. 6. Heavy-mineral results for all the sections (see location in Fig. 2), with the stratigraphic log of each section (A: San Juan de la Peña sedtion; B: Peña Oroel section; C: Jaca section; D: Santa Orosia section; E: Canciás section) and position of the analyzed samples and the occurrence of petrofacies (modified from Roigé et al., 2017). Squares, dots, triangles and rhombs correspond to petrographic samples studied in previous works (Roigé et al. 2016, 2017). F) Color legend used for heavy-mineral pie diagrams. G) Ternary diagram used for petrofacies discrimination (data from Roigé et al., 2018).

Fig. 7. Correspondence analysis of the heavy-mineral compositions displayed as biplots. A) Biplot of raw data where Ep: epidote; Tur: Tourmaline; Zrn: zircón; Rt: rutile; Ap: apatite; Grs: grossular; Alm: Almandine; Ttn: titanite; Cld: chloritoid; Fo: forsterite; Mz: monazite; Cpx: clinopyroxene; St: staurolite; Svn: svanbergite; Act: actinolite; Xtm: xenotime; Ves: vesuvianite: Ky: kyanite; Sp: spinel; Sph: sphalerite. B) Biplot of data treated according to correlations shown by the raw data analysis. C) Biplot of heavy-mineral compositions of sedimentary environments. D) Biplot of heavy-mineral compositions of petrofacies. E) Biplot of heavy-mineral compositions of sedimentary units. In Parts B, C, D, and E Ap: Ap+Cld+Sph; ZTR: Zrn+Tur+Rt; OtHM: Alm+Grs+Ttn+Ves+Cpx+Act+St+Ky+Xtm+Svn; Fo.Sp: Fo+Sp; Ep:Ep.

Fig. 8. A) Clinopyroxene from the Rapitán channel displaying no signs of advanced corrosion features. B) Almadine from the Rapitán channel displaying no signs of corrosion. C) Staurolite from the Rapitán channel displaying no signs of corrosion. D) Tourmaline from the Banastón turbidite system displaying no signs of corrosion. E) Zircon from the Banastón turbidite system displaying no signs of corrosion. F)

Rutile from the Banastón turbidite system displaying no signs of corrosion. G) Almandine from the lower Jaca turbidite system displaying advanced dissolution features. H) Apatite from the Rapitán channel displaying no signs of corrosion. I) Zircon from the Banastón turbidite system displaying no signs of corrosion.

Fig. 9. A) Olivine from the Belsué-Atarés delta displaying no signs of intense corrosion. B) Almadine from the Sabiñanigo Sandstone displaying no signs of corrosion. C) Olivine from the Santa Orosia alluvial fan displaying no signs of intense corrosion. D) Grossular from the Sabiánigo Sandstone displaying no signs of corrosion. E) Clinopyroxene from the Santa Orosia alluvial fan displaying slight corrosion. F) Staurolite from the Sabiñanigo Sandstone displaying no signs of corrosion.

Fig. 10. A) Tourmaline from the Canciás fan displaying slight to advanced degree of corrosion. B) Apatite from the Canciás fan displaying slight to advanced degree of corrosion.

Fig. 11. A) Clinopyroxene from the Belsué-Atarés delta displaying no signs of intense corrosion. B) Clinopyroxene from the Belsué-Atarés delta displaying slight degree of corrosion. C) Almandine from the Belsué-Atarés delta displaying no signs of intense corrosion. D) Grossular from the Belsué-Atarés delta displaying no signs of intense corrosion. E) Staurolite from the Belsué-Atarés delta displaying no signs of intense corrosion. F) Clinopyroxene from the fluvial Campodarbe Formation displaying no signs of intense corrosion.

Table 1. Results of the counting expressed as relative abundances of heavy minerals. Banastón TS: Banastón Turbidite Sytem; Jaca TS: Jaca Turbidite System; Rap C: Rapitán Channel; Sabiñánigo: Sabiñánigo Sandstone; Belsué: Belsué-Atarés Fm.; Camp: Campodarbe Group; Sta. Orosia fan: Santa Orosia fan; Canciás fan: Canciás fan; Oroel fan: Peña Oroel fan; S. Juan de la Peña fan: San Juan de la Peña fan; CEE: "Carbonate extrabasinal enriched" petrofacies; SD: "Siliciclastic dominant" petrofacies; HCD: "Hybrid-clast-dominated" petrofacies; MLC: "Mixed lithic and carbonate" petrofacies; Petrofacies data from Roigé et al. (2018); Ep: epidote; Tur: Tourmaline; Zrn: zircón; Rt: rutile; Ap: apatite; Grs: grossular; Alm: Almandine; Ttn: titanite; Cld: chloritoid; Fo: forsterite; Mz: monazite; Cpx: clinopyroxene; St: staurolite; Svn: svanbergite; Act: actinolite; Xtm: xenotime; Ves: vesuvianite: Ky: kyanite; Sp: spinel; Sph: sphalerite.

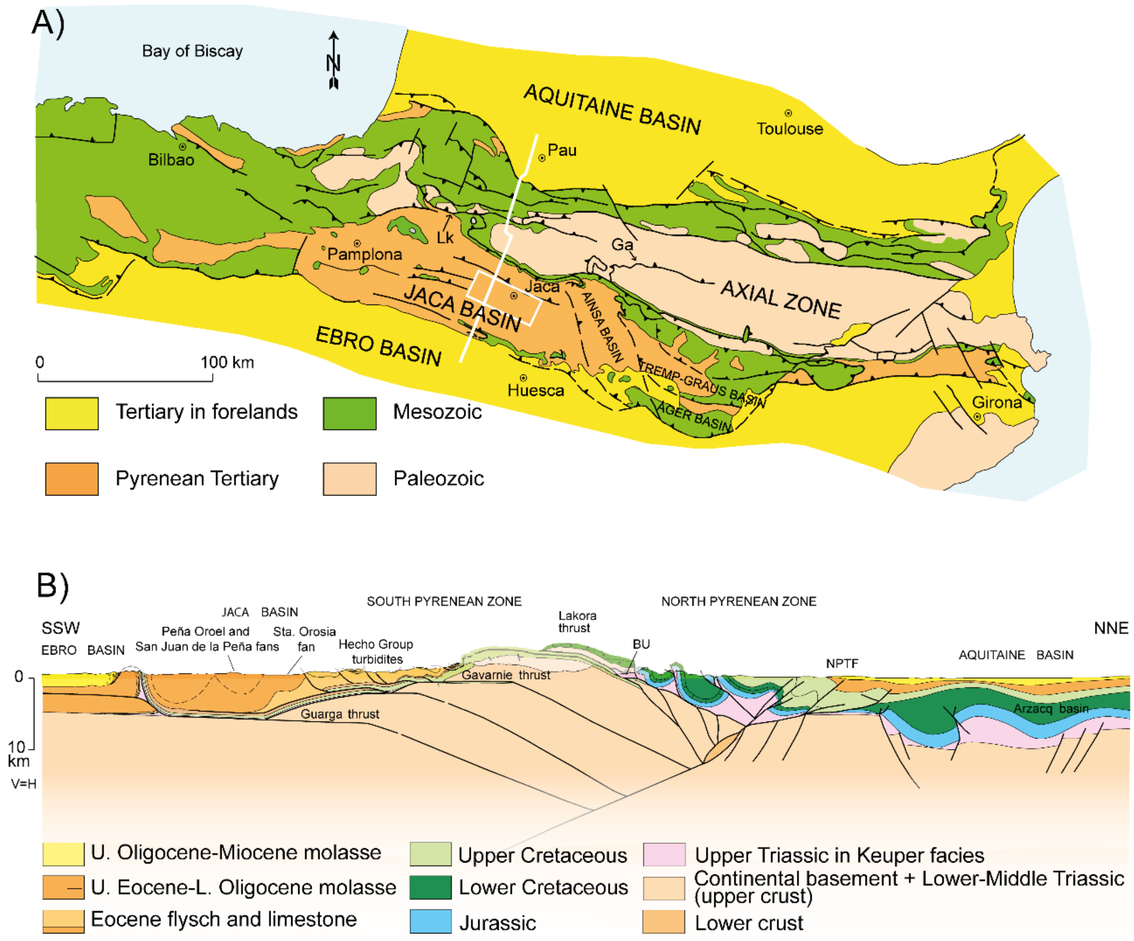
A)
Bay of Biscay
N
AQUITAINE BASIN
Toulouse
Pau
Bilbao
Lk
Pamplona
Ga
AXIAL ZONE
Jaca
JACA BASIN
AINSA BASIN
EBRO BASIN
TREMP-GRAUS BASIN
AGER BASIN
Huesca
Girona
0
100 km
Tertiary in forelands
Mesozoic
Pyrenean Tertiary
Paleozoic
B)
SSW
EBRO BASIN
JACA BASIN
Peña Oroel and San Juan de la Peña fans
Sta. Orosia fan
Hecho Group turbidites
SOUTH PYRENEAN ZONE
Lakora thrust
BU
NORTH PYRENEAN ZONE
NPTF
AQUITAINE BASIN
NNE
Gavarnie thrust
Guarga thrust
Arzacq basin
0
10 km
V=H
U. Oligocene-Miocene molasse
U. Eocene-L. Oligocene molasse
Eocene flysch and limestone
Upper Cretaceous
Lower Cretaceous
Jurassic
Upper Triassic in Keuper facies
Continental basement + Lower-Middle Triassic (upper crust)
Lower crust

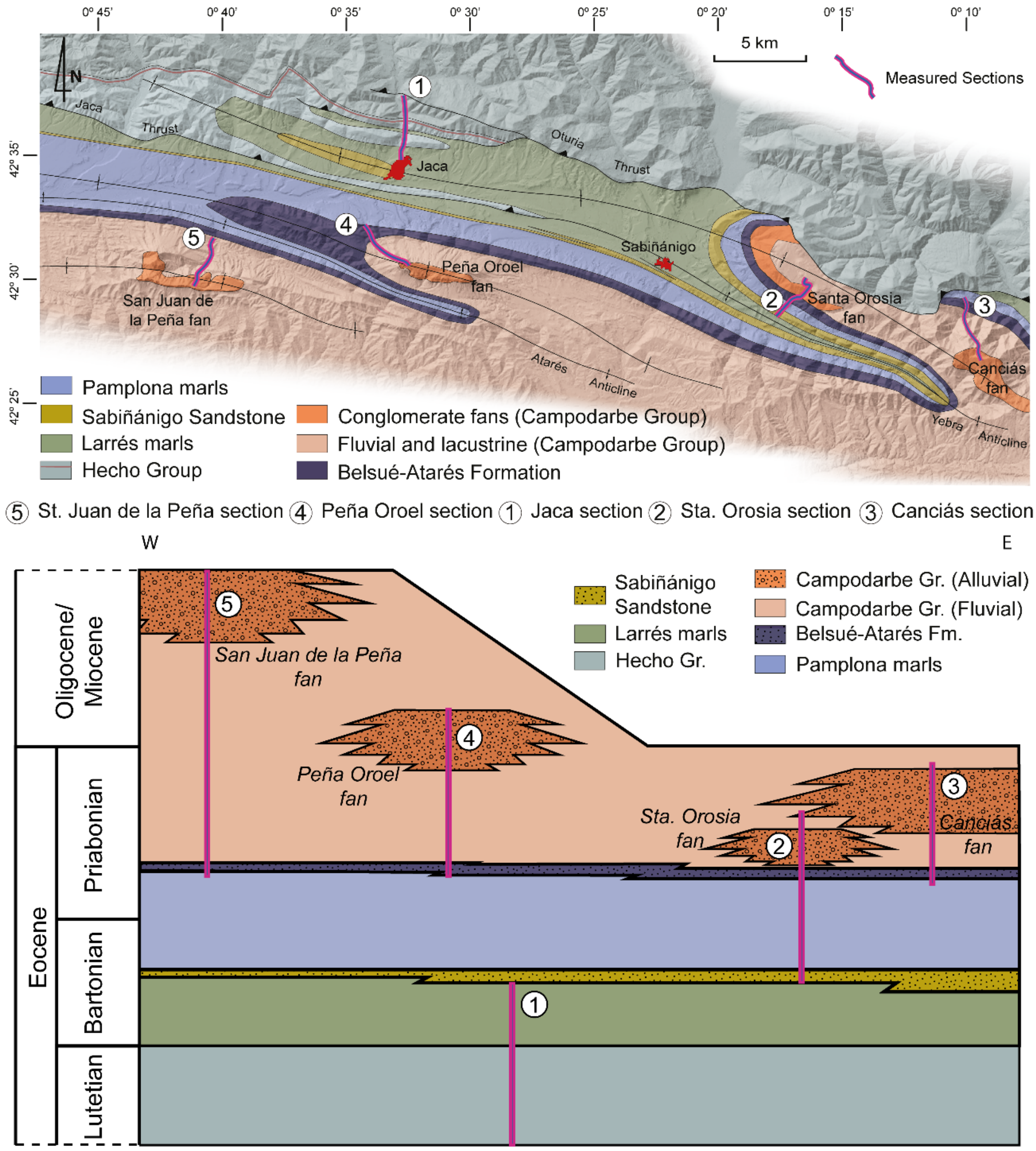

0° 45'
0° 40'
0° 35'
0° 30'
0° 25'
0° 20'
0° 15'
0° 10'
42° 35'
42° 30'
42° 25'
N
5 km
Measured Sections
Jaca
Thrust
Oturia
Thrust
Jaca
Sabiñánigo
Peña Oroel
fan
San Juan de
la Peña fan
Santa Orosia
fan
Canciás
fan
Atarés
Anticline
Yebra
Anticline
Pamplona marls
Sabiñánigo Sandstone
Larrés marls
Hecho Group
Conglomerate fans (Campodarbe Group)
Fluvial and lacustrine (Campodarbe Group)
Belsué-Atarés Formation
5 St. Juan de la Peña section 4 Peña Oroel section 1 Jaca section 2 Sta. Orosia section 3 Canciás section
W
E
Oligocene/
Miocene
Eocene
Priabonian
Bartonian
Lutetian
San Juan de la Peña
fan
Peña Oroel
fan
Sta. Orosia
fan
Canciás
fan
Sabiñánigo
Sandstone
Larrés marls
Hecho Gr.
Campodarbe Gr. (Alluvial)
Campodarbe Gr. (Fluvial)
Belsué-Atarés Fm.
Pamplona marls

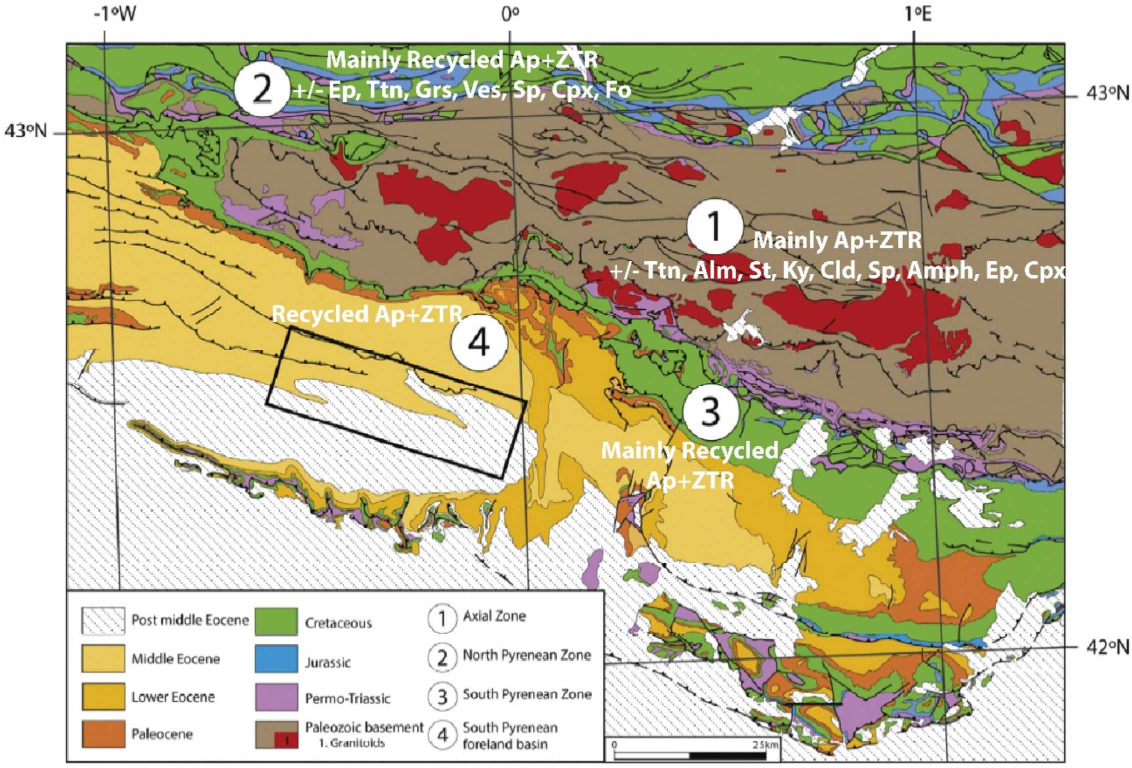
-1ºW
0º
1ºE
43ºN
43ºN
42ºN
Mainly Recycled Ap+ZTR
+/- Ep, Ttn, Grs, Ves, Sp, Cpx, Fo
2
1
Mainly Ap+ZTR
+/- Ttn, Alm, St, Ky, Cld, Sp, Amph, Ep, Cpx
Recycled Ap+ZTR
4
3
Mainly Recycled
Ap+ZTR
Post middle Eocene
Middle Eocene
Lower Eocene
Paleocene
Cretaceous
Jurassic
Permo-Triassic
Paleozoic basement
1. Granitoids
1 Axial Zone
2 North Pyrenean Zone
3 South Pyrenean Zone
4 South Pyrenean foreland basin
0
25km

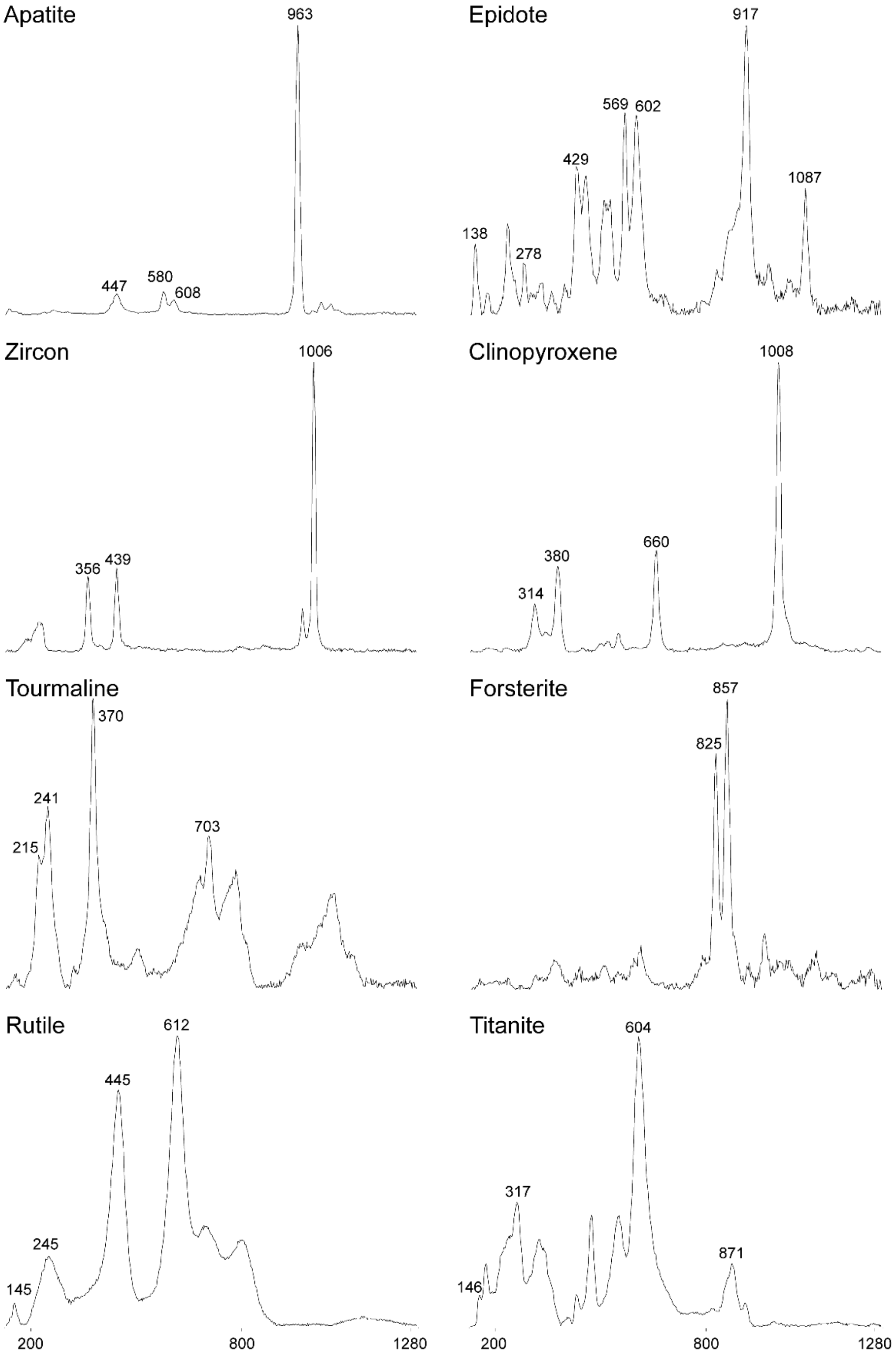
Apatite
963
447
580
608
Epidote
917
569
602
429
1087
138
278
Zircon
1006
356
439
Clinopyroxene
1008
660
380
314
Tourmaline
370
241
215
703
Forsterite
857
825
Rutile
612
445
245
145
Titanite
604
317
871
146
200
800
1280
200
800
1280

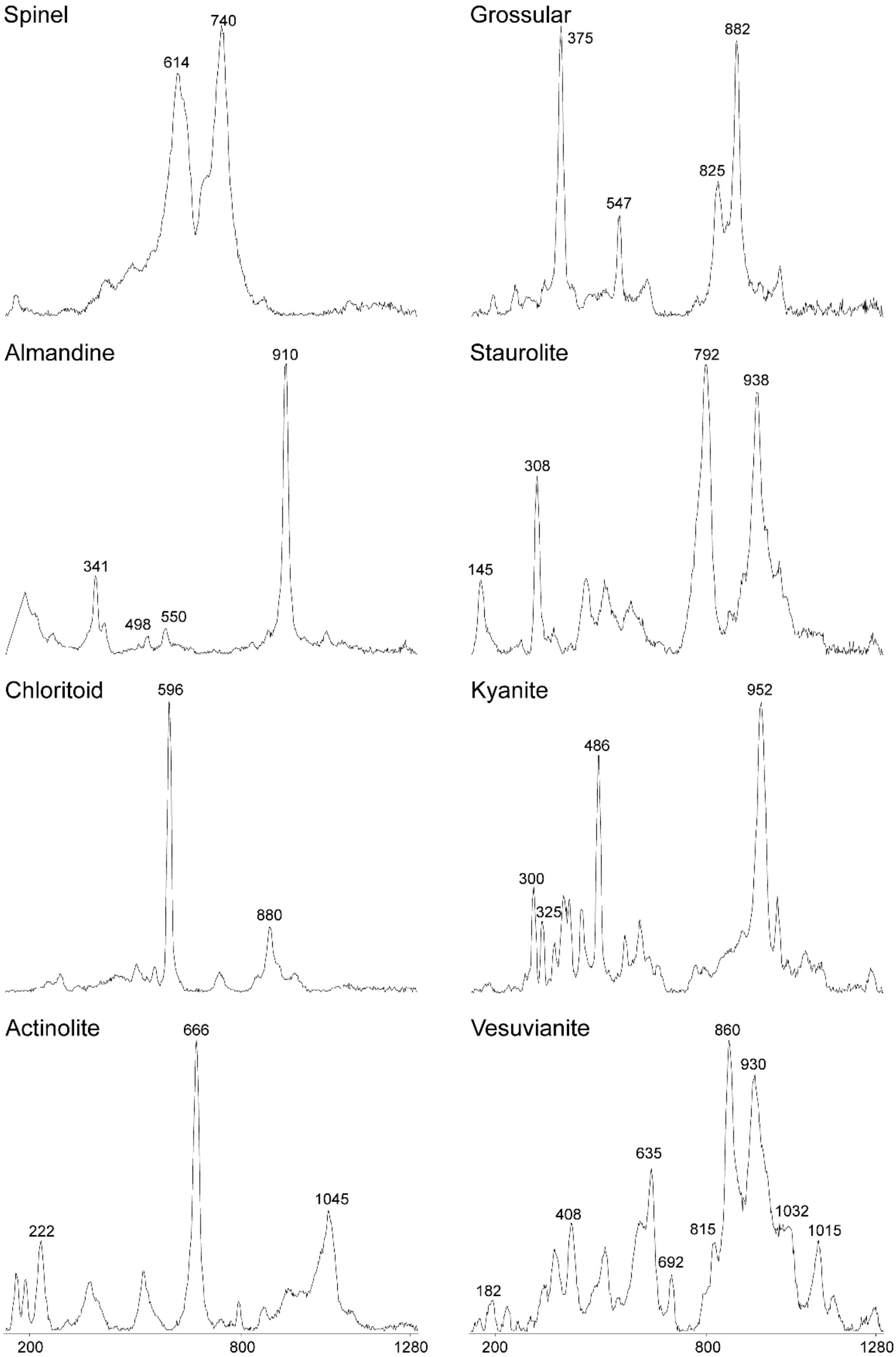
Spinel
614
740
Grossular
375
547
825
882
Almandine
341
498
550
910
Staurolite
145
308
792
938
Chloritoid
596
880
Kyanite
300
325
486
952
Actinolite
222
666
1045
Vesuvianite
182
408
635
692
815
860
930
1032
1015
200
800
1280
200
800
1280

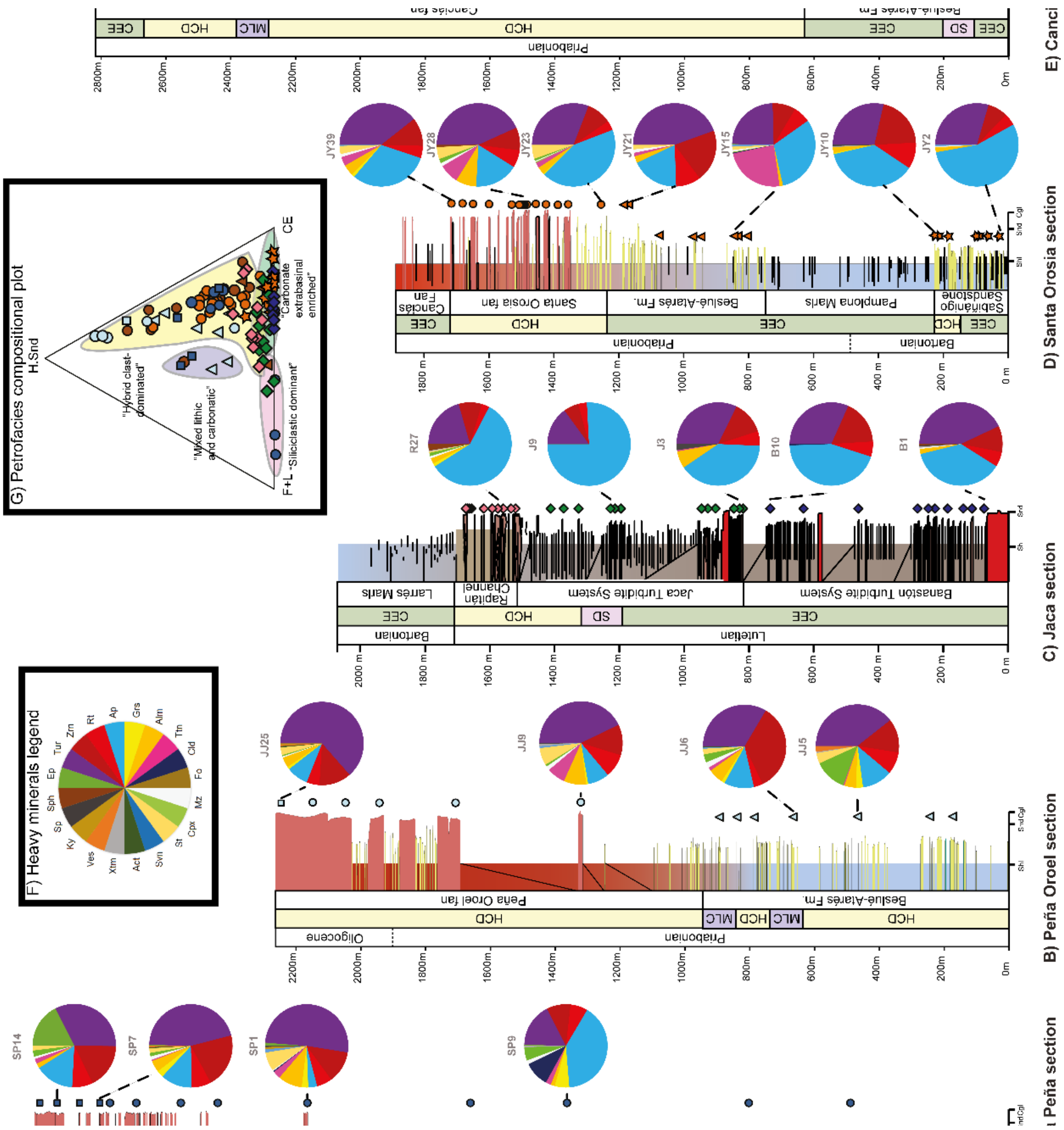
G) Petrofacies compositional plot
H.Snd
F+L
CE
"Hybrid clast-dominated"
"Mixed lithic and carbonatic"
"Siliciclastic dominant"
"Carbonate extrabasinal enriched"
F) Heavy minerals legend
B) Peña Oroel section
C) Jaca section
D) Santa Orosia section
E) Canci
Priabonian
Bartonian
Lutetian
Oligocene
Peña Oroel fan
Besilué-Atarés Fm.
Banastón Turbidite System
Jaca Turbidite System
Rapitán Channel
Larrés Marls
Pamplona Marls
Sabiñánigo Sandstone
Santa Orosia fan
Cancías fan

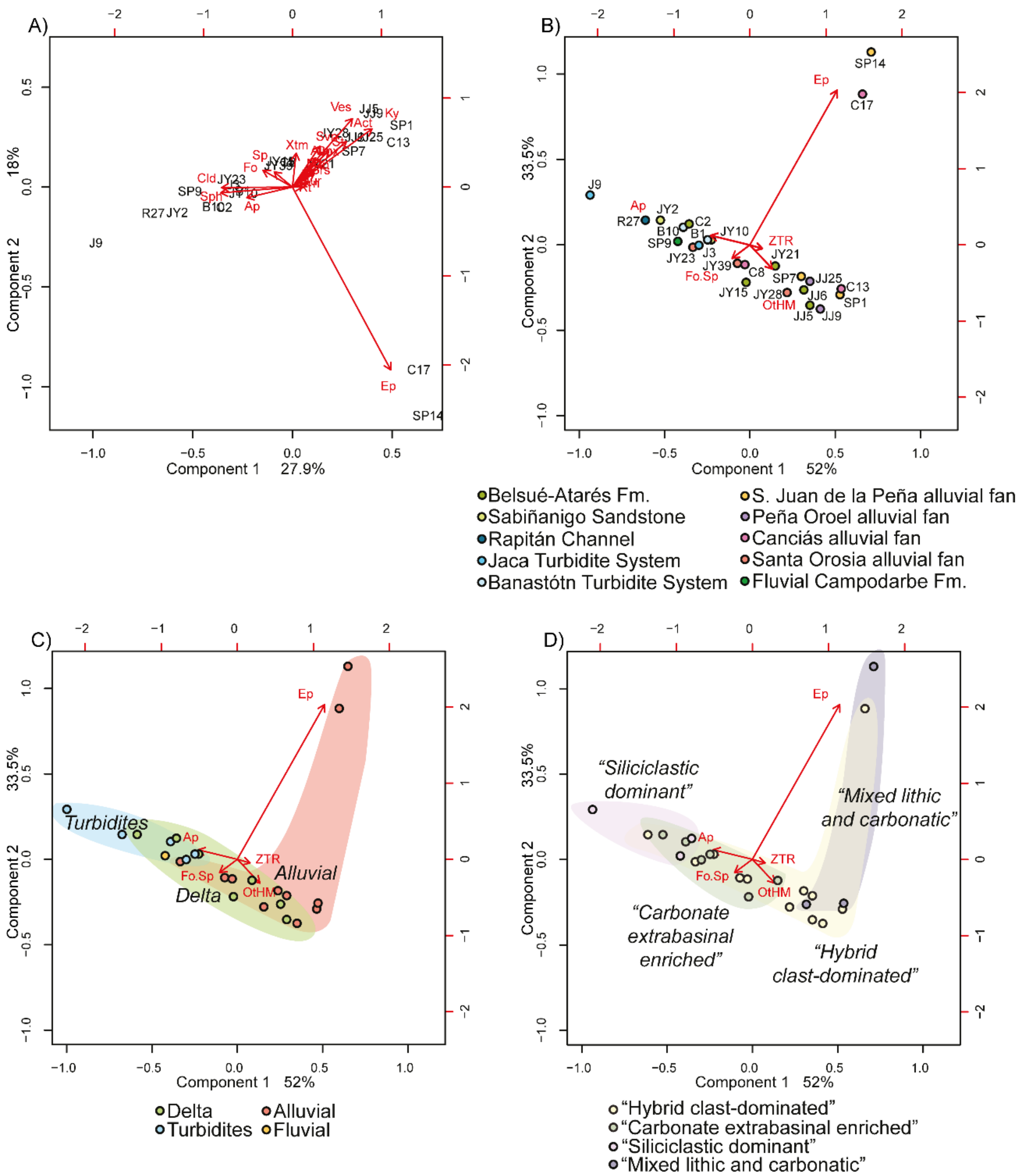
A)
B)
C)
D)
Component 1 27.9%
Component 2 18%
Component 1 52%
Component 2 33.5%
Ep
Ap
ZTR
Fo.Sp
OtHM
Belsué-Atarés Fm.
Sabiñanigo Sandstone
Rapitán Channel
Jaca Turbidite System
Banastótn Turbidite System
S. Juan de la Peña alluvial fan
Peña Oroel alluvial fan
Canciás alluvial fan
Santa Orosia alluvial fan
Fluvial Campodarbe Fm.
Turbidites
Delta
Alluvial
Fluvial
"Siliciclastic dominant"
"Mixed lithic and carbonatic"
"Carbonate extrabasinal enriched"
"Hybrid clast-dominated"

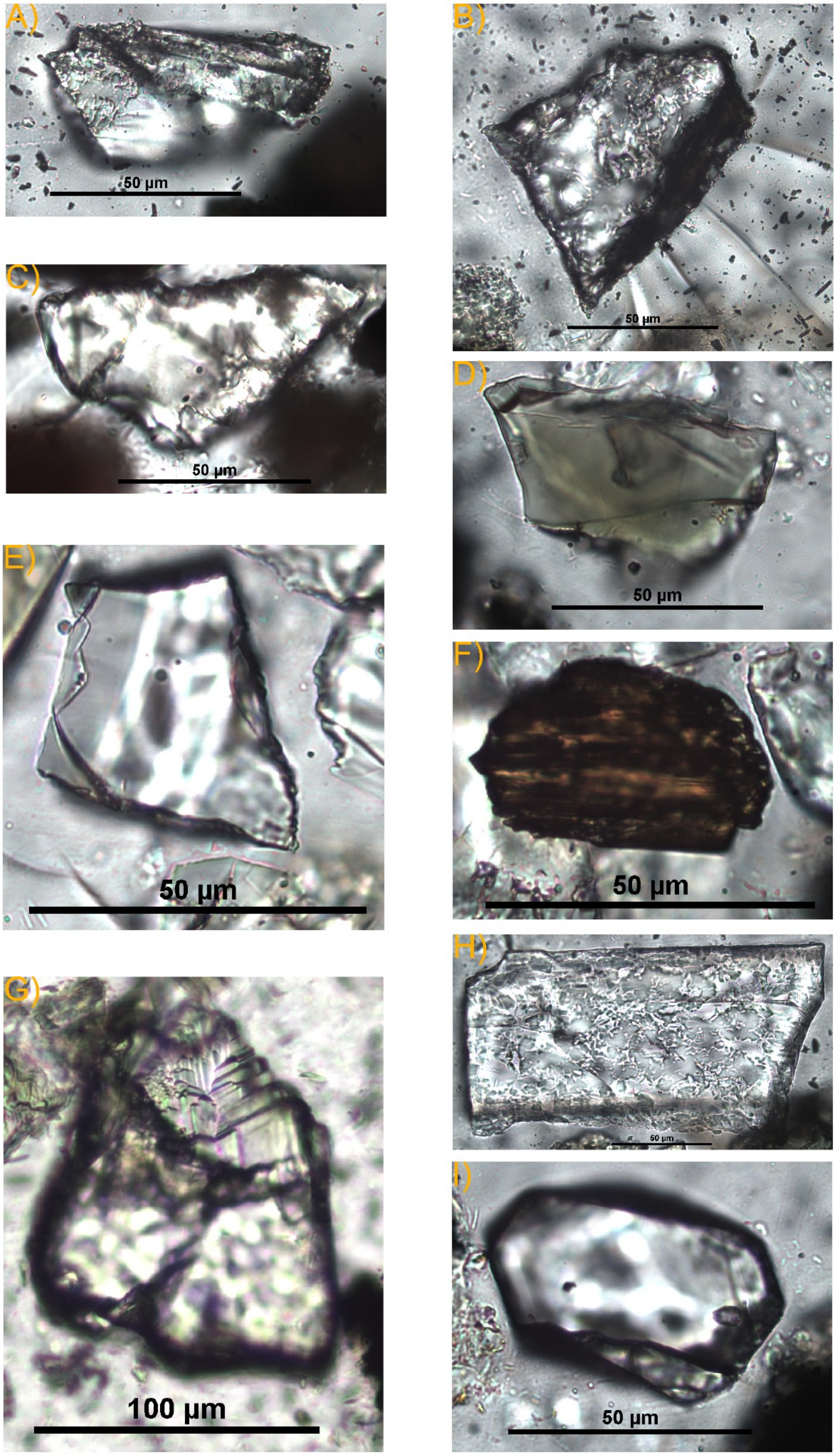
A)
50 µm
B)
50 µm
C)
50 µm
D)
50 µm
E)
50 µm
F)
50 µm
G)
100 µm
H)
50 µm
I)
50 µm

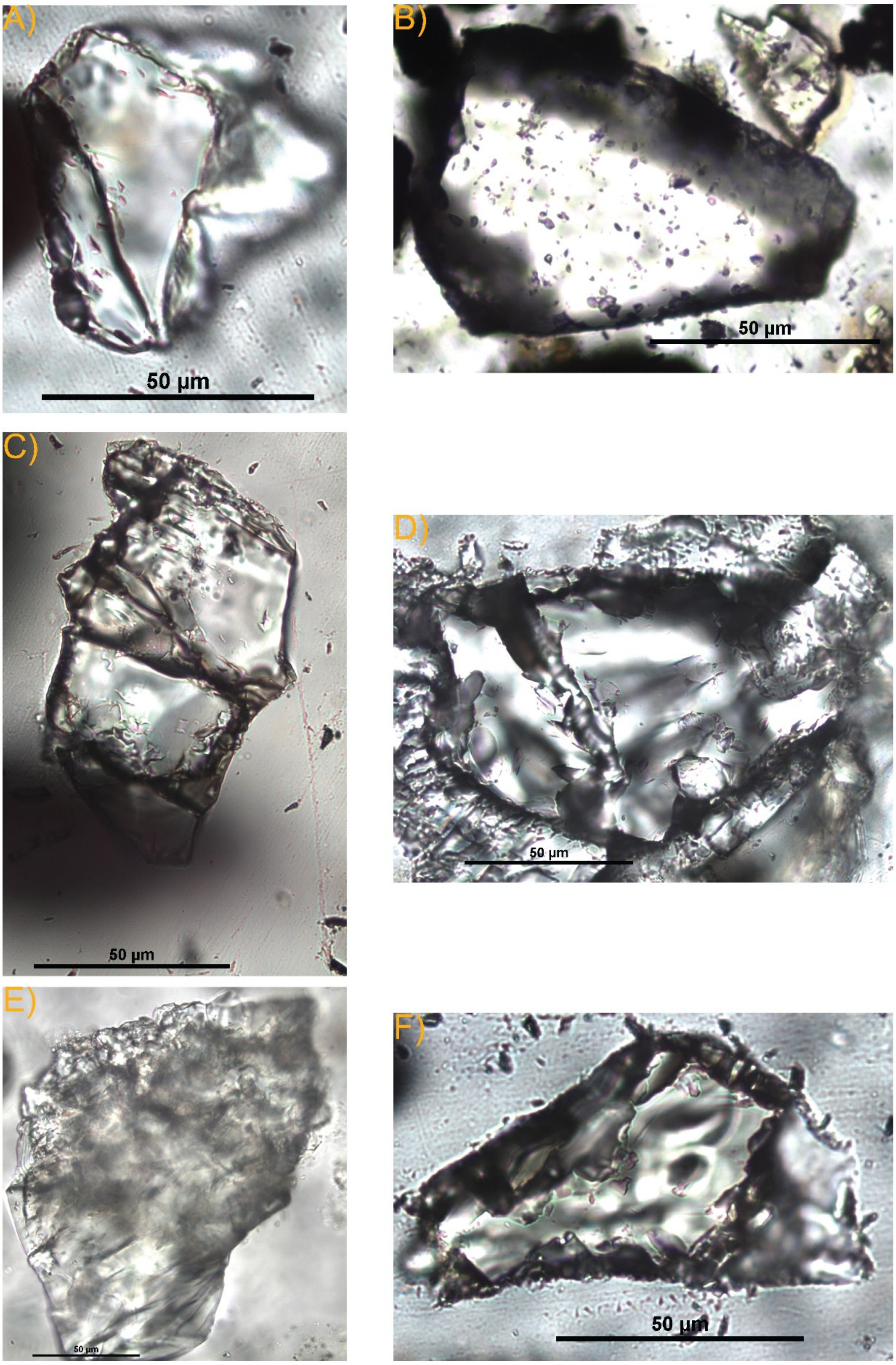
A)
50 µm
B)
50 µm
C)
50 µm
D)
50 µm
E)
F)
50 µm

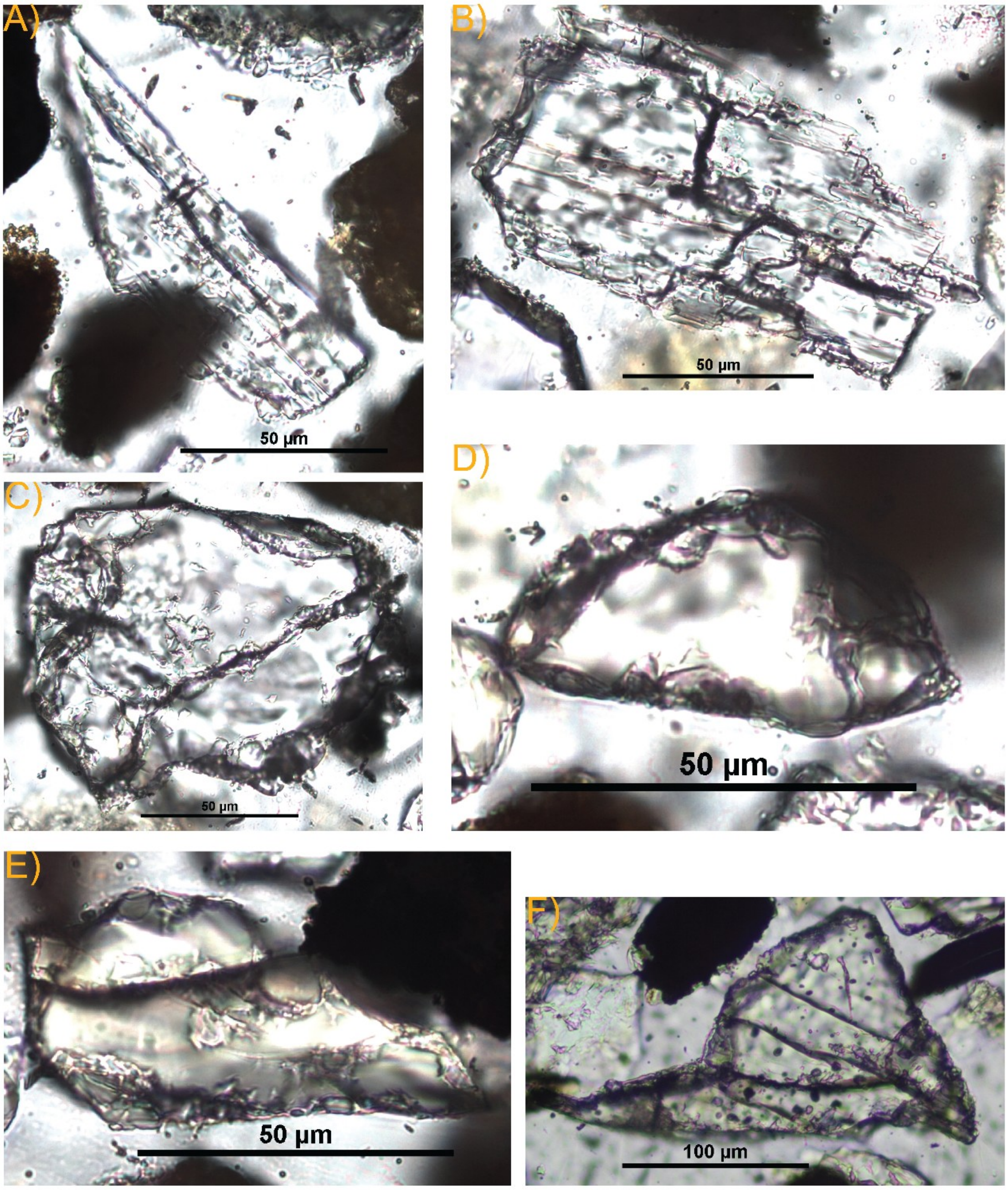
A)
50 μm
B)
50 μm
C)
50 μm
D)
50 μm
E)
50 μm
F)
100 μm

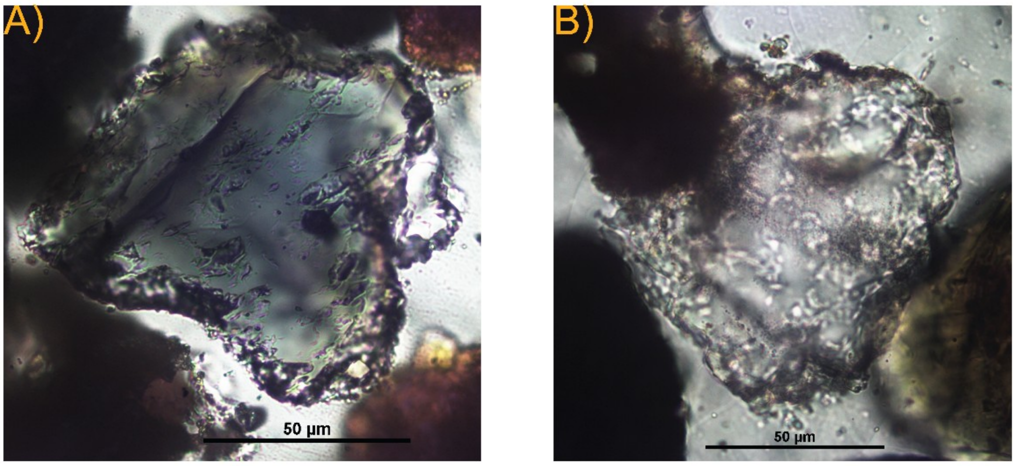
A)
50 µm
B)
50 µm